https://doi.org/10.5194/egusphere-2025-2828
Preprint. Discussion started: 8 July 2025
© Author(s) 2025. CC BY 4.0 License.

Distinct mechanisms shaping global surface and root-zone soil moisture

Zijun Wang[1], Rong Wu[2], Yangyang Liu[3], Chenfeng Cui[1], Na Zhao[4], Yinghan Zhao[3], Zhongming Wen[3], Zhixin Zhang[3], Wei Zhang[3]

Correspondence to: Yangyang Liu (hnlylcbtks@163.com)

[1] College of Water Resources and Architectural Engineering, Northwest A&F University, Yangling, Shaanxi 712100, China
[2] School of Environmental Science and Engineering, Southern University of Science and Technology, Shenzhen, Guangdong 518055, China
[3] College of Grassland Agriculture, Northwest A&F University, Yangling, Shaanxi 712100, China
[4] State Key Laboratory of Resources and Environmental Information System, Institute of Geographic Sciences and Natural Resources Research, Chinese Academy of Sciences, Beijing 100101, China

https://doi.org/10.5194/egusphere-2025-2828
Preprint. Discussion started: 8 July 2025
© Author(s) 2025. CC BY 4.0 License.

Abstract: Soil moisture (SM) plays a vital role in the global water and carbon cycles, with long-term impacts on ecosystem functioning and vegetation growth. However, under the background of climate change, a decoupling phenomenon have occurred between surface soil moisture (SMsurf) and rootzone soil moisture (SMroot). The variations and primary driving factors of SM across different layers have not been studied comprehensively. Therefore, this study explored the spatiotemporal dynamics of global SMsurf and SMroot from 2001 to 2021. The Random Forest coupled with numerical simulation experiments were applied to measure the influences of climate and vegetation dynamics to SM changes. The Partial Least Squares Structural Equation Modeling was employed to demonstrate the direct and indirect pathways of them to SM variability. Additionally, the copula functions were applied to examine the probability of SM loss under different stress scenarios caused by climate or vegetation changes. The results indicated that SM variation exhibited a significant spatial heterogeneity. Global greening significantly contributed to the increase in SMsurf at a rate of 0.000087 $m^3/m^3/a$, while precipitation (Pre) had the most significant impact on replenishing SMroot, with a contribution rate of 0.000117 $m^3/m^3/a$. Atmospheric water demand (Ep) was identified as the primary cause of global SM drought, with rates of -0.000089 $m^3/m^3/a$ and -0.000075 $m^3/m^3/a$ for SMsurf and SMroot respectively. Although vapor pressure deficit (VPD) had a significant dominant effect in regions with high VPD values, rather than globally, as global positive and negative VPD effects offset each other. Vegetation typically acted as an intermediary variable transmitting the indirect effects of climate factors on SM. Under the extreme scenarios, Precipitation, Standardized precipitation evapotranspiration index and vegetation resulted in the highest probability of SM loss. This research will furnish a theoretical underpinning for global water resource management and hold significant implications for the sustainable development of ecosystems.

Short summary:

This study explores global soil moisture changes from 2001 to 2021, revealing the distinct response mechanisms of surface and rootzone layers from both a contribution and probability perspective. Climate factors and vegetation both affect soil moisture, with precipitation and vegetation playing key roles in maintaining balance. The research highlights rising drought risks due to increased atmospheric demand and offers insights to support global water management and ecosystem sustainability.

Keywords:

Soil moisture; vegetation greening; climate change; drought stress; probabilistic threshold

https://doi.org/10.5194/egusphere-2025-2828
Preprint. Discussion started: 8 July 2025
© Author(s) 2025. CC BY 4.0 License.

1. Introduction

Soil moisture (SM) constitutes a vital element within the soil-vegetation-atmosphere continuum (Berdugo et al., 2020; Liu et al., 2020b; Wang et al., 2017; Zhou et al., 2021a; Jung et al., 2010b), governing the transfer of water, carbon, and energy fluxes between terrestrial ecosystems and the atmosphere (Vereecken et al., 2014; Legates et al., 2011), playing an indispensable role in preserving the stability of the agricultural ecosystem. Compared to the total global water resources, although the quantity of SM may seem insignificant, its dynamics critically induce large CO_2 fluxes (about two to three gigatons of carbon per year) (Green et al., 2019). More importantly, SM exhibits distinct functional stratification: Surface soil moisture (SMsurf) dominates short-term hydrological processes by controlling rainfall partitioning into infiltration versus runoff (Feng and Zhang, 2015), while root-zone soil moisture (SMroot) regulates vegetation water uptake and ecosystem resilience, and influences carbon assimilation, community succession and biogeochemical cycles (Hirschi et al., 2014b; Yang et al., 2022).

Traditional in-situ observations have demonstrated substantial variability in the driving factors of SM dynamics across different spatial scales, temporal periods, and soil depths (Huang et al., 2016; Duan et al., 2016). Huang et al. (2016) revealed that the controlling factors of SM differ significantly across soil depths in the Wulongchi catchment. Based on slope-scale observations in the Loess Plateau, Duan et al. (2016) demonstrated that SM is predominantly controlled by a combination of topographic and soil characteristics at both hillslope and landscape scales. However, due to the difficulty of obtaining dense and long-term SM observations from in-situ networks on a global scale, these datasets may not be representative at large spatial scales (Guan et al., 2023). With the advancement and improvement of remote sensing technologies and SM retrieval algorithms, global monitoring of SM dynamics has become increasingly feasible. Nevertheless, accurately estimating SMroot remains challenging, as most remote sensing satellites primarily capture moisture in the near-surface layer (Feng, 2016) , such as ESA CCI (European Space Agency Climate Change Initiative) (Gruber et al., 2019; Dorigo et al., 2017). The emergence of reanalysis datasets, such as ERA5 (the land component of the fifth generation of European Reanalysis), and land surface model-based products such as GLEAM (Global Land Evaporation Amsterdam Model) and GLDAS (Global Land Data Assimilation System), has helped fill the long-standing gap in global SMroot data and is widely employed in hydrometeorological studies(Yuan et al., 2023; Zhang et al., 2025).

SMsurf has received widespread attention in previous studies due to its observational accessibility and rapid response to atmospheric forcings such as precipitation and temperature (Feng and Zhang, 2015; Deng et al., 2020a). Global-scale analyses have consistently reported sustained decreases in SMsurf across 73% of vegetated lands since 1988, particularly in mid-latitude drylands (Dorigo et al., 2012). ESA CCI SM confirmed the "Dry Gets Drier, Wet Gets Wetter" (DGDWGW) paradigm (Feng and Zhang, 2015); however, this pattern was derived solely from SMsurf observations and did not account for the dynamics

https://doi.org/10.5194/egusphere-2025-2828
Preprint. Discussion started: 8 July 2025
© Author(s) 2025. CC BY 4.0 License.

of SMroot. The factors driving the SMsurf changing trends have also been extensively and thoroughly studied. Deng et al. (2020a) revealed that the declining trend in SMsurf is primarily driven by global temperature increases. Cho and Choi (2014) demonstrated SMsurf are dominantly regulated by precipitation and temperature/radiation. The development of land data assimilation techniques and land surface models has enabled large-scale investigations of SMroot. Globally, SMroot has decreased at an average rate of 0.14×10^{-3} m^3/m^3/year, primarily attributed to temperature anomalies (Luo et al., 2023).

Intensifying land-atmosphere hydrological interactions have positioned climate forcing as a dominant regulator of SM dynamics under climate change (Bonan, 2008). Moreover, climate change not only directly influences SM availability and vegetation patterns but also modulates SM dynamics through vegetation-mediated feedback mechanisms. Emerging evidence highlights vegetation serves as a crucial intermediary between climatic forcing and SM responses (Zhang et al., 2022a; Yang et al., 2023). There exists a pronounced mutual constraint between vegetation and SM. Favorable climatic conditions promote vegetation growth; however, increased vegetation cover simultaneously intensifies SM consumption, potentially exacerbating soil drought. In turn, soil drought imposes constraints on vegetation growth, creating a feedback loop that regulates ecosystem dynamics (Lian et al., 2020; Zhu et al., 2016; Tietjen et al., 2017). Ruichen et al. (2023a) revealed that the increase in vegetation cover has generally diminished the responsiveness of SM to precipitation fluctuations in most regions. However, in regions with abundant vegetation cover, enhanced evapotranspiration has instead led to greater SM responsiveness to climate change. Some studies suggested that in water-limited areas, vegetation greening and increased productivity accelerate soil evaporation, depleting SM (Yang et al., 2014; Jung et al., 2010b; Aragao, 2012; Jasechko et al., 2013; Seneviratne et al., 2010b; Li et al., 2018). However, other research indicated that regional-scale interannual precipitation changes compensate for the depletion of SM caused by vegetation cover and increased productivity (Xie et al., 2015; Meng et al., 2020). Despite numerous studies has emphasized the variability of SM across multiple spatial and temporal scales, and highlighted the critical roles of climate change and vegetation dynamics in shaping SM variability, the quantitative assessment of the contributions of climate and vegetation change and their interaction to SM dynamics at different layers remains unclear.

As the rapid-response layer of the climate system, SMsurf primarily regulates surface energy balance and the daily fluctuations of evapotranspiration. In contrast, SMroot, functioning as a slow-regulation layer, exerts profound seasonal influences on vegetation productivity, root distribution patterns, and belowground carbon allocation (Seneviratne et al., 2010a; Jung et al., 2010a).. Though SMsurf and SMroot exhibit strong hydraulic connectivity through vertical water redistribution via infiltration and plant root systems (Vereecken et al., 2022), recent studies reveal that climate change is decoupling the different layers of SM. Specifically, SM dynamics across different soil layers exhibit different change trends and the dominant driving factors may also vary, especially under climate change, which further complicating our comprehension of soil moisture-climate-vegetation interactions (Zhou et al., 2021b; Hirschi et al., 2014a). Hirschi et al. (2014a) found that SMsurf gradually

https://doi.org/10.5194/egusphere-2025-2828
Preprint. Discussion started: 8 July 2025
© Author(s) 2025. CC BY 4.0 License.

becomes statistically decoupled from both SMroot and atmospheric conditions under drought conditions, by comparing the temporal variability of in situ observations of SMsurf and SMroot. Luo et al. (2023) also observed a negative correlation between SMsurf and SMroot in many parts of the world, particularly in high northern latitudes and arid regions such as central and western Australia. Several regional-scale studies have further confirmed the decoupling between SMsurf and SMroot. For example, Li et al. (2021a) found that SMsurf in the Loess Plateau is more sensitive to short-term climatic variables such as precipitation and potential evapotranspiration, as well as vegetation cover, whereas SMroot is more significantly influenced by long-term factors such as vegetation type (e.g., water use by deep-rooted plants) and global atmospheric circulation patterns (e.g., ENSO). In East Asia, Zohaib et al. (2017) demonstrated that reduced precipitation is the primary cause of SMsurf decline, while Cheng et al. (2015) highlighted that the dominant factors affecting SMroot vary across different climatic regions. Furthermore, the distinct variation trends of SMsurf and SMroot, as well as their driving mechanisms of climate and vegetation changes, have not been comprehensively examined, particularly considering the significant spatial heterogeneity across different climate zones. Additionally, the probability of SM deficits triggered by vegetation dynamics and climate change remains unexplored, which is crucial for optimizing agricultural irrigation strategies and maintaining the stability of agricultural ecosystems under climate change. Therefore, it is necessary to clarify these interaction mechanisms and assess the collaborative effects and comparative contributions of climate change and vegetation dynamics on SM at a global scale, which benefit for better comprehension of these processes will enhance our understanding of the complex interactions among climate, vegetation, and SM across diverse climatic regions.

Previous studies have paid less attention to the changing trends and driving mechanism of SMsurf and SMroot under climate change and vegetation dynamics, especially across the different climatic zones globally. At the same time, the probability of SM extremes when abnormal situations occur among the influencing factors are inadequately resolved. Consequently, this study aims to (1) characterize the spatiotemporal dynamics of SMsurf and SMroot under distinct climatic regions, (2) measure the relative contributions of climate change and vegetation greening to SM fluctuations based on random forest coupled numerical simulation experiments, (3) elucidate both direct and indirect pathways through which vegetation dynamics and climatic variables regulate SM changes based on structural equation models, and (4) assess the sensitivity thresholds of SM responses to multifactorial drivers under coupled environmental interactions based on copula functions. This research will help understand soil hydrological processes and provide a theoretical basis for global water resources management.

https://doi.org/10.5194/egusphere-2025-2828
Preprint. Discussion started: 8 July 2025
© Author(s) 2025. CC BY 4.0 License.

2. Materials and methods

2.1. Data sources and processing

2.1.1 Köppen-Geiger climate classification data

The Köppen-Geiger climate classification, first proposed by Vladimir Köppen in 1884, is one of the most widely used systems for categorizing global climates. It provides a valuable framework for analyzing climate distribution and predicting regional climate characteristics. To examine the temporal variations of SM across different climate zones at both global and regional scales, this study utilized the Köppen-Geiger climate classification map (Beck et al., 2018), which has a spatial resolution of 0.5° × 0.5° and covers the period from 1980 to 2016. Following Luo et al. (2023), this study further grouped the detailed climate zones into five broad categories: polar, boreal, temperate, arid, and tropical (Figure. 1).

2.1.2. Soil moisture

The Global Land Evaporation Amsterdam Model (GLEAM) SM dataset offers high-quality, spatially continuous estimates of surface (0–10 cm) and root-zone (10–250 cm) SM (http://gleam.eu/). With a high spatiotemporal resolution of 0.1° at a daily scale since 1980, it is driven by a combination of satellite observations and reanalysis-based forcings, ensuring reliable and consistent SM assessments across diverse regions (Miralles et al., 2011; Martens et al., 2017a). GLEAM SM data has been applied in several researches in both global and regional contexts (Li et al., 2021c; Ye et al., 2019; Xu et al., 2023; Ruichen et al., 2023b; Zhang et al., 2022b). Benefiting from an improved representation of evaporative stress, an optimized water-balance module, and a refined SM data assimilation strategy, GLEAM SM offers enhanced accuracy and reliability, with a 0.1° spatial resolution and monthly time resolution, covering January 2001 - December 2021.

The Global Land Data Assimilation System (GLDAS), developed by National Aeronautics and Space Administration (NASA) Goddard Space Flight Center, is a comprehensive hydrological modeling framework designed to synthesize multi-source observational data (satellite remote sensing and in situ measurements) with advanced land surface models (Noah, CLM, VIC, Mosaic, and Catchment land surface models) and data assimilation techniques (https://disc.gsfc.nasa.gov/). GLDAS generates vertically stratified SM estimates across four depth layers (0-10 cm, 10-40 cm, 40-100 cm, and 100-200 cm), which serve as crucial basic supporting data for meteorological, land surface and hydrological research. This study utilized GLDAS_NOAH025_M SM data with a spatiotemporal resolution of 0.25° at a month scale from January 2001 to December 2021.

ERA5-Land, the most advanced reanalysis dataset from the European Centre for Medium-Range Weather Forecasts (ECMWF), is accessible via the Copernicus Climate Change Service (C3S) Climate Data Store (CDS) (https://cds.climate.copernicus.eu/), which offers a total of 50 variables and depict the water and energy cycles over land

https://doi.org/10.5194/egusphere-2025-2828
Preprint. Discussion started: 8 July 2025
© Author(s) 2025. CC BY 4.0 License.

globally. This study utilized ERA5-Land at one month interval and with a 0.25° spatial resolution, which include a four-layer vertical profile ranging from 0–7 cm to 100–289 cm, covering from January 2001 to December 2021.

GLEAM SM was rigorously validated through extensive field SM measurements (e.g., International Soil Moisture Network), confirming its strong performance in capturing SM dynamics in different regions (Martens et al., 2017b). In order to enhance the stability of results, this research further evaluates the accuracy of the GLEAM SM product at both surface and root-zone depths. To ensure consistency across multiple SM datasets, a weighted averaging method was employed to standardize SM measurements to a uniform depth. Considering that SM values typically have small magnitudes, this research uses relative root mean square error (RRMSE) and Pearson correlation coefficient (R) as evaluation metrics to offer a more stringent and scientifically sound assessment of GLEAM SM. The results indicated that GLEAM exhibited high consistency with both GLDAS and ERA5, with a global mean RRMSE of less than 20% and R of around 0.6 (Figure. S2, Figure. S3). The agreement between SMsurf and other datasets is slightly stronger than that of SMroot. Specially, the global RRMSE results are great. Only south edge areas in Tibetan Plateau and Sahara Desert own the very unsatisfactory results (Figure. S2). The correlation coefficients between GLEAM and other datasets are relatively low in high-latitude regions of the Northern Hemisphere, averaging around 0.5, but they increase to 0.8 or even above 0.9 south of 60°N (Figure. S3).

2.1.3. Vegetation parameters

The Global Land Surface Satellites (GLASS) provided the Leaf Area Index (LAI) based on satellite data from multiple remote sensing sensors like Moderate Resolution Imaging Spectroradiometer (MODIS) and Advanced Very High Resolution Radiometer (AVHRR). The data had a spatial resolution of 0.25° and an 8 - day temporal resolution. Owe to sophisticated processing and model inversion, this dataset has been widely used in ecological and hydrological research fields with high spatiotemporal resolution globally (Xiao et al., 2016; Li and Xiao, 2020; Xiao et al., 2017; Wang et al., 2014; Zeng et al., 2017; Wei et al., 2017). This study utilized the LAI dataset derived from the MODIS sensor with a spatial resolution of 0.25° and an 8-day interval (http://www.glass.umd.edu/).

Significant progress has been made in measuring terrestrial photosynthesis via Solar-Induced Fluorescence (SIF). SIF shows a strong relationship with Gross Primary Productivity (GPP) data (Li and Xiao, 2019). The Global OCO-2 SIF dataset (GOSIF) was further developed through data - driven methods, incorporating discrete OCO - 2 SIF detections, MODIS remote sensing data, and meteorological reanalysis data, and has seen extensive application (Zhang et al., 2022b; Chang et al., 2023). This study utilized the average global GOSIF-Gpp from 2001 to 2021, with a spatial resolution of 0.05° and a monthly temporal resolution from January 2001 to December 2021. (http://data.globalecology.unh.edu/data/GOSIF-GPP_v2/).

https://doi.org/10.5194/egusphere-2025-2828
Preprint. Discussion started: 8 July 2025
© Author(s) 2025. CC BY 4.0 License.

2.1.4. Climatic variables

The meteorological data for this study were obtained from the GLDAS_NOAH025_M data product, boasting a spatial resolution of 0.25° and a monthly temporal resolution. GLDAS provide a variety of critical land surface parameters, such as downward longwave radiation (Lrad), downward shortwave radiation (Srad), atmospheric pressure, specific humidity, precipitation (Pre), atmospheric water demand (Ep), temperature (Temp), and wind speed (WS).

For this study, the total radiation (Rad) was computed based on the original data, in accordance with Eq.1:

$$Rad = LRad + SRad \quad (1)$$

Where Rad represents the total radiation; $LRad$ stands for the longwave downward radiation; and $SRad$ denotes the shortwave downward radiation.

VPD was estimated based on Eq.2 and Eq.3:

$$RH = 0.263pq\left[e^{\left(\frac{17.67(T-T_0)}{T-29.65}\right)}\right]^{-1} \quad (2)$$

$$VPD = 0.61078 \times e^{\frac{17.27\times(T-273.16)}{T-273.16+237.3}} \times (1 - RH) \quad (3)$$

Where RH is Relative humidity, p is the atmospheric pressure (Pa); q is specific humidity (dimensionless); T is the Temp (K); T_0 is the reference Temp (273.16 K usually).

In order to further investigate the impact of global teleconnection factors such as NAO (North Atlantic Oscillation), PDO (Pacific Decadal Oscillation), AO (Arctic Oscillation), and ENSO (El Niño - Southern Oscillation) on SM. This study obtained teleconnection factors sourced from the National Centers for Environmental Information (https://www.ncei.noaa.gov/) (Zhao et al., 2020).

2.1.5. SPEI

The Standardized Precipitation Evapotranspiration Index (SPEI) is used to assess Meteorological drought conditions. By incorporating the cumulative effects of long-term climate variability rather than merely reflecting single-month conditions, the SPEI can characterize the degree of water deficit (the difference between precipitation and evapotranspiration) and capture the delayed responses of vegetation cover and SM to water deficit, for instance, spring droughts may not be directly caused by insufficient rainfall in that month but rather by a prolonged precipitation deficit from the previous autumn (Jiao et al., 2021). Given that vegetation growth and SM variations often lag behind climatic conditions by several months, the 12-month moving average of SPEI better aligns with the ecological inertia of these processes, rather than directly corresponding to instantaneous precipitation or evapotranspiration (Xu et al., 2023), which is of great significance for monitoring and predicting the impact of climate change on agricultural water resources management and agricultural ecosystem. The SPEI from the Global SPEI

https://doi.org/10.5194/egusphere-2025-2828
Preprint. Discussion started: 8 July 2025
© Author(s) 2025. CC BY 4.0 License.

database with a spatial resolution of 0.5° and a temporal scale of 12 months, were used in this study (https://spei.csic.es/spei_database) (Beguería et al., 2014).

2.1.6. Pre-processing of datasets

Bilinear interpolation was used to interpolate all data to a spatial resolution of 0.25° (Li et al., 2022). To aggregate the 8-day time-scale LAI data into monthly values, the maximum value method was utilized.

Trends are often regarded as indicative of human activity, suggesting that non-stationary conditions could potentially distort the results inappropriately (Boulton et al., 2022). Therefore, prior to subsequent calculations, it is essential to eliminate the trend from the SM time series (Smith and Boers, 2023). This study employed the STL (Seasonal and Trend decomposition using Loess) method to separate SM time series of each grid cell into the overall trend, seasonal component, and residual component, which was implemented through the *stl()* function in the "stats" package in R (v4.2.1). The STL residual component, which represents the deseasonalized and detrended SM time series, was utilized for further analysis (Wang et al., 2023). Taking global observational results as an example, although the mean values of the three SM products exhibited substantial differences, their dynamic fluctuation patterns showed a high degree of consistency (Figure. S4a, b). After STL decomposition, the detrended and deseasonalized residual components demonstrated near-uniform synchronicity (Figure. S4c, d), indicating that STL not only eliminated the effects of non-stationary conditions but also effectively removed systematic biases among products. This ensured the reliability of subsequent analytical results.

2.2. Methods

2.2.1. Trend analysis

Theil-Sen slope estimation and Mann-Kendall (MK) test were used to identify and characterize trends in long-term time series data. The Theil-Sen method was utilized for calculating resilient linear trends with p-values that are robust against outliers (Gocic and Trajkovic, 2013). Simultaneously, the non-parametric MK test was applied to evaluate the significance of monotonic trends through the assessment of their slope values (Ma et al., 2020).

2.2.2. Numerical simulation experiments based on Random Forests

Random Forest (RF) has demonstrated favorable performance in simulating SM by capturing non-linear associations among variables (Breiman, 2001; Clewley et al., 2017; Li et al., 2021d; Liu et al., 2020c; Zhao et al., 2018). Due to the limitations of traditional physical models in representing input parameters, this study employed an RF-based surrogate model to simulate SM and subsequently conducted numerical experiments to separate the absolute contributions of different variables (Zhao et al., 2022). R^2 and RMSE were used to evaluate the simulation results of RF.

https://doi.org/10.5194/egusphere-2025-2828
Preprint. Discussion started: 8 July 2025
© Author(s) 2025. CC BY 4.0 License.

The Feature Importance Index (FII) derived from RF quantitatively described the relative contributions of input features. Traditional control variable experiments or numerical simulations were typically based on physical models and were constrained by predefined input variables. This study has integrated the strengths of both approaches to propose numerical simulation experiments based on RF. The selected independent variables as shown in Table 1.

The specific approach to separating variable contributions using this method is as follows:

1. Input Actual Time-Series Data: real time-series data for all independent variables were input into RF model to simulate the dependent variable (SMsurf and SMroot), and the hyperparameters of the model were optimized using Bayesian algorithms.

2. Fix a Specific Variable: one specific variable (e.g., LAI) was fixed in 2001, while the rest of the variables remain time-varying, and the hyperparameters were the same as those from Step 1.

3. Run Two Simulations: Since the data inputs differ between the two simulations, the difference between the two simulation outputs could be attributed to the contribution of LAI to SM (details in Table 1 and Figure. S5).

The dominant factors of global SM were further identified. Specifically, this study simultaneously considered the contributions of and the changing trends of each factor and SM. For regions where SM increased, the factor with the highest positive contribution was determined as the dominant factor, and vice versa (Sun et al., 2022).

Table 1. Description of numerical simulation experiments.

Experiments	Description
E_{all}	All variables remain time-varying
E_{LAI}	LAI is fixed in 2001 while the rest of variables remain time-varying
E_{SIFGpp}	SIFGPP is fixed in 2001 while the rest of variables remain time-varying
E_{SPEI}	SPEI is fixed in 2001 while the rest of variables remain time-varying
E_{Pre}	Pre is fixed in 2001 while the rest of variables remain time-varying
E_{Ep}	Ep is fixed in 2001 while the rest of variables remain time-varying
E_{VPD}	VPD is fixed in 2001 while the rest of variables remain time-varying
E_{Temp}	Temp is fixed in 2001 while the rest of variables remain time-varying
E_{Rad}	Rad is fixed in 2001 while the rest of variables remain time-varying
E_{WS}	WS is fixed in 2001 while the rest of variables remain time-varying

2.2.3. PLS-SEM

Partial Least Squares Structural Equation Modeling (PLS-SEM) is a robust and versatile multivariate analysis technique that has increasingly been applied in fields such as ecology and hydrology. In this study, PLS-SEM was employed to investigate the direct and indirect influence pathways of meteorological factors and vegetation on SM. Unlike covariance-based SEM (CB-SEM), PLS-SEM does not rely on strict normality assumptions and can be applied with relatively small sample sizes,

https://doi.org/10.5194/egusphere-2025-2828
Preprint. Discussion started: 8 July 2025
© Author(s) 2025. CC BY 4.0 License.

making it especially useful in exploratory research where theoretical models are less established (Hair et al., 2016). In this study, the PLS-SEM analysis was carried out using SmartPLS 3.3.1, a widely recognized software tool designed to implement this technique efficiently (Westland, 2015; Thomson et al., 1995). The software enables bootstrapping procedures to assess the significance of paths and estimates in the model, thus providing a semi-parametric method for hypothesis testing. This methodological framework offers both explanatory and predictive capabilities, allowing the researchers to explore complex relationships between observed and latent variables, contributing to the robustness and reliability of the findings (Deng et al., 2020b; Zani et al., 2020).

2.2.4. Wavelet coherence analysis

Wavelet coherence analysis is a time-frequency analysis method based on wavelet transform, which is used to study the mutual relationship and frequency coupling between two signals. By applying wavelet transform to each signal and calculating their coherence at different time and frequency scales, wavelet coherence analysis can reveal the time-frequency interactions and coherence level between two signals. This analysis method has been widely applied in fields such as meteorology and hydrology, aiding in the exploration of complex frequency characteristics and interaction mechanisms between signals (Torrence and Compo, 1998; Hu and Si, 2016; Li et al., 2021b). In this study, wavelet coherence analysis was employed to investigate the correlation between global teleconnection factors and SM.

2.2.5. Copula functions

Copula functions, a robust mathematical approach, are being used more and more in ecology and hydrology. They are employed to depict and model the tail dependencies among multiple variables (Wu et al., 2025), particularly those exhibiting complex, non-linear relationships (Qing et al., 2023; Zscheischler and Seneviratne, 2017). Sklar's theorem is the foundation of copula theory. It posits that any multivariate distribution can be broken down into its marginal distributions and a copula, which represents the dependence structure (Sklar, 1959). Various types of copulas, like Gaussian, t-copula, Clayton, Gumbel, and Frank—are applied in hydrological scenarios to capture different types of dependence, covering both symmetric and asymmetric dependences (Genest and Favre, 2007).

This study selected the optimal copula function from five copula functions and constructed a bivariate dependence function to characterize the joint distribution of SM and independent factors (details in Table S1). Taking Temp as an example, the corresponding joint distribution is expressed as follows:

$$F_{SM,Temp}(sm, temp) = P(SM \leq \mathrm{sm}^{n-th}, Temp \geq \mathrm{temp}^{n-th}) = C\left(F_1(\mathrm{sm}), F_2(\mathrm{temp})\right) \quad (6)$$

Where, $C(\,)$ denotes a copula function. $F_1(\mathrm{sm}^{n-th})$ and $F_2(\mathrm{vpd}^{n-th})$ represent the marginal distributions of SM and Temp, respectively.

https://doi.org/10.5194/egusphere-2025-2828
Preprint. Discussion started: 8 July 2025
© Author(s) 2025. CC BY 4.0 License.

The performance of the Copula function is assessed through the squared Euclidean distance d (i.e. the difference between the probabilities obtained from each Copula function and those from the empirical Copula function), calculated as follows:

$$d = \sum_{i=1}^{n} |C_{emp}(F_1(\mathrm{sm}), F_2(\mathrm{temp})) - C_k(F_1(\mathrm{sm}), F_2(\mathrm{temp}))|^2 \quad (7)$$

Based on the determined joint distribution function, we calculated the joint conditional probabilities of different levels of SM deficiency under different stress scenarios, that is, moderate, severe, and extreme scenarios. These were defined as the time series of factors being located at the 50th, 30th, and 10th percentiles, respectively, which were unfavorable for maintaining SM. Taking the Temp of a certain pixel as an example, when sorting the time series from small to large, the minimum value was located at the 0th percentile, and the maximum value was located at the 100th percentile. Assuming that high Temp were unfavorable for maintaining SM, extreme Temp scenarios occurred when the temperature exceeded the 10th percentile of the time series. Subsequently, we used the magnitude of the joint conditional probabilities to indicate the sensitivity of SM to Temp. Taking SM deficiency under different temperature scenarios as an example, the calculation of conditional probabilities is as shown in Eq.7:

$$P(u_1 < \mathrm{SM} \leqslant u_2 | \mathrm{Temp} \geq \mathrm{temp}^{10th}) = \frac{P(u_1 < \mathrm{SM} \leqslant u_2, \mathrm{Temp} \geq \mathrm{temp}^{10th})}{P(\mathrm{Temp} \geq \mathrm{temp}^{10th})} = \frac{F_{\mathrm{SM,\ Temp}}(u_2, \mathrm{temp}^{10th}) - F_{\mathrm{SM,\ Temp}}(u_1, \mathrm{temp}^{10th})}{F_{\mathrm{SM}} u_2 - F_{\mathrm{SM}} u_1} \quad (8)$$

Where, temp^{10th} represents temperatures within the top 10th percentile, u_1 and u_2 are the upper and lower limits of SM, $F_{\mathrm{SM,\ Temp}}$denotes the joint distribution of the two variables, with F_{SM} being the marginal distribution of SM.

3. Results

3.1. Spatiotemporal variations of SM

The spatiotemporal dynamics of global SM exhibited pronounced spatial heterogeneity (Figure. 1). While the spatial variation rates of SMsurf and SMroot were relatively similar (Figure. S6), discrepancies emerge in hotspot regions of SM change (Figure. 1). Specifically, the mean values of SMsurf and SMroot differed significantly in the Northern Hemisphere, whereas they remained nearly identical in the Southern Hemisphere. Furthermore, our study revealed that in hotspot regions of SM change, SMsurf exhibited greater fluctuations compared to SMroot. Notable declining trends were observed across central North America, Central and Eastern Europe, the Central Siberian Plateau, the Brazilian and Paraná Plateaus, the Congo Basin in Central Africa, and northwestern Australia. Conversely, significant increases were detected in northwestern Europe, the West Siberian Plain, Central East Asia, the Indian subcontinent, and the southeastern region of the Great Artesian Basin, with maximum rates exceeding 0.002 $m^3/m^3/a$ (Figure. 1). From a latitudinal perspective, the most pronounced increase in SM occurred between 30°N and 40°N, whereas the most substantial decline was concentrated around 20°S. Longitudinally, regions

https://doi.org/10.5194/egusphere-2025-2828
Preprint. Discussion started: 8 July 2025
© Author(s) 2025. CC BY 4.0 License.

316 near 120°W, 60°E, and 120°E exhibited the highest rates of increase. The detailed description of the spatiotemporal variations
317 in vegetation indicators, drought indicators, and climate factors can be found in Text S1 and Figure. S7–S15.
318
319
320

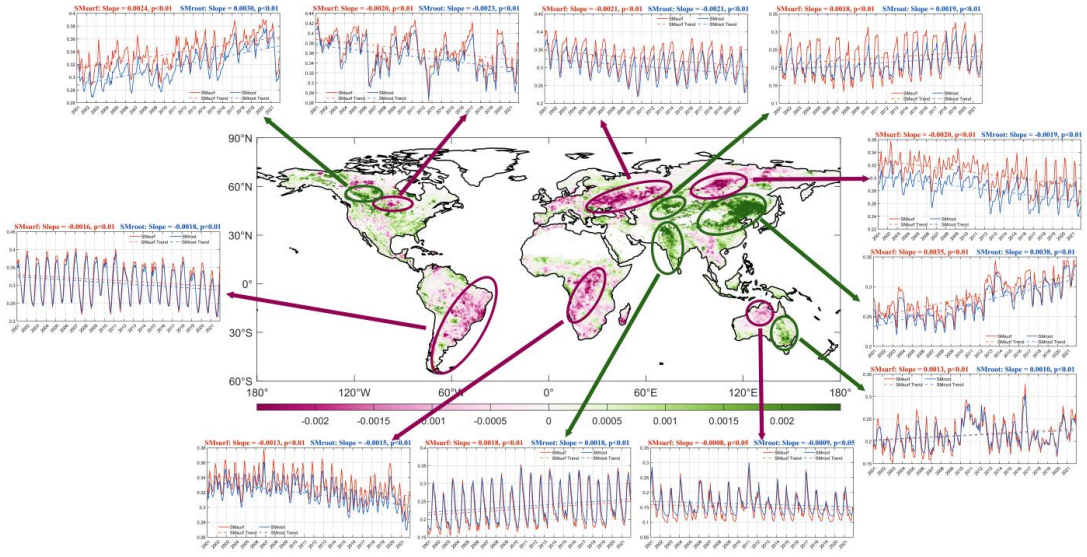

321
322 Figure. 1. Spatiotemporal Trends of SM from 2001 to 2021. The red polyline in the line chart represents SMsurf, while the
323 blue polyline represents SMroot.
324

325 **3.2. Contributions of vegetation indicators, drought indicator and climate factors to SM variations**

326 RF-based numerical simulation experiments were conducted to measure the contributions of various factors to SM, with
327 the model demonstrating good performance (Figure. S16). Figure. 2 indicated significant regional differences in the
328 contributions of different factors to SM, with Pre, Ep, and VPD playing a relatively large role. Pre had a strong positive
329 contribution to SM in the Guiana Highlands, the Western Ghats, the Northeast China Plain and the North China Plain, reaching
330 up to 0.0008 $m^3/m^3/a$. However, it had a negative contribution of up to -0.0006 $m^3/m^3/a$ in the Kara-Kum Desert, the Australian
331 Basin, the Paraná Plateau, and southeastern China. Ep showed a negative contribution of up to -0.0008 $m^3/m^3/a$ in the
332 Australian Basin, south of the West Siberian Plain, the Mongolian Plateau, the North American Great Plains, and the Chad
333 Basin, while exhibiting a prominent positive contribution in Europe, vegetation-covered areas of the Sahara Desert, the Arabian
334 Peninsula, the Congo Basin, and south of the Yangtze River in China. VPD had a significant negative contribution to SM
335 between 30°S and 30°N, but a positive contribution in higher latitude regions. Additionally, LAI had a significant positive

https://doi.org/10.5194/egusphere-2025-2828
Preprint. Discussion started: 8 July 2025
© Author(s) 2025. CC BY 4.0 License.

336 contribution in the Congo Basin, the Amazon Basin, and south of the Himalayas, while exhibiting a large negative contribution
337 in the Guinea Gulf region, the Mississippi Plain, the Orinoco Plain, the Brazilian Plateau, the Indian Peninsula, the Indochina
338 Peninsula, and eastern and central parts of China. WS had a substantial positive contribution in the Qinghai-Tibet Plateau,
339 while the contributions of Temp and Rad showed less spatial variation. Overall, the magnitude and direction of contributions
340 varied for different climate zones and globally. From a global perspective, LAI and Rad increased SMsurf but decreased
341 SMroot, while Pre decreased SMsurf but increased SMroot (Figure. 3).

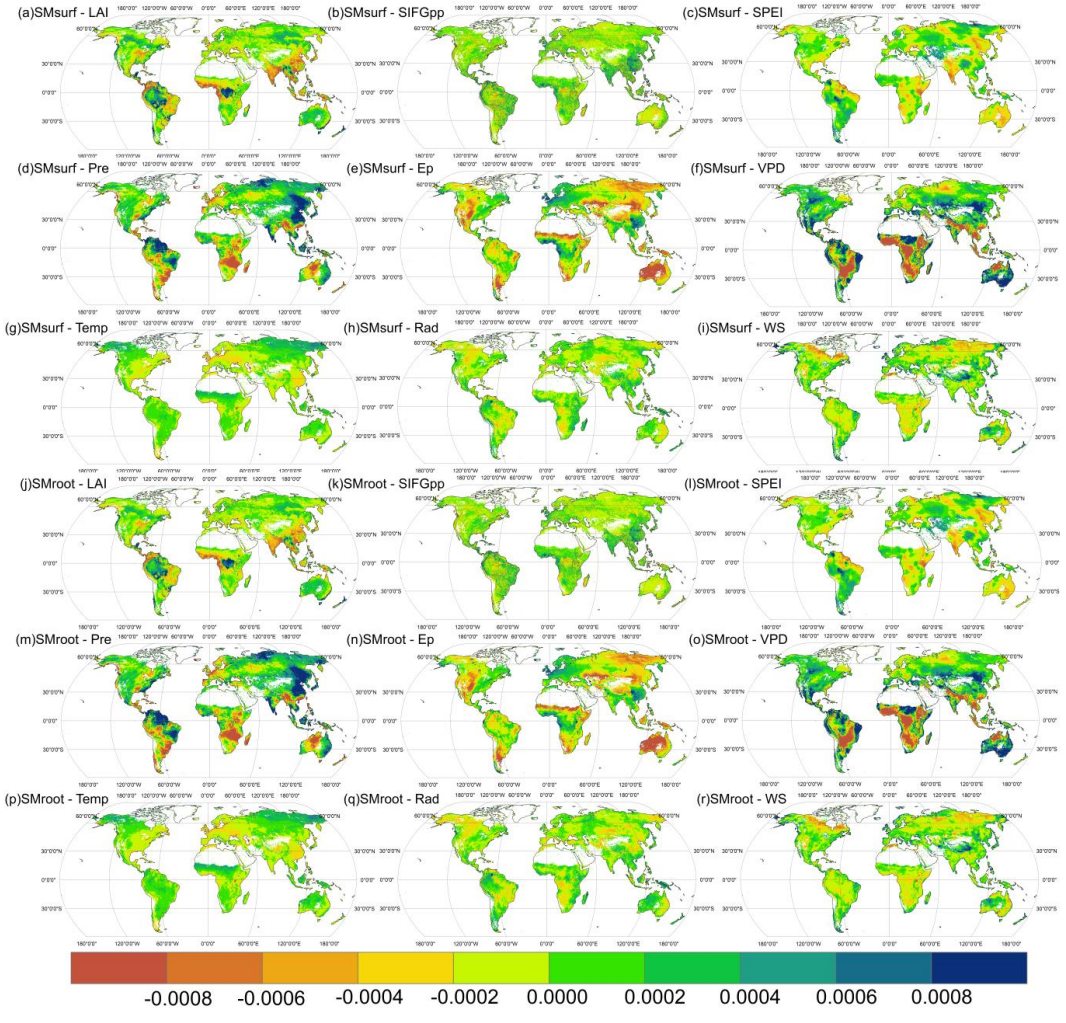

342

343 Figure. 2. Spatial distribution of absolute contribution of vegetation characteristics, climate factors, and drought indices to
344 SMsurf and SMroot ($m^3/m^3/a$).

https://doi.org/10.5194/egusphere-2025-2828
Preprint. Discussion started: 8 July 2025
© Author(s) 2025. CC BY 4.0 License.

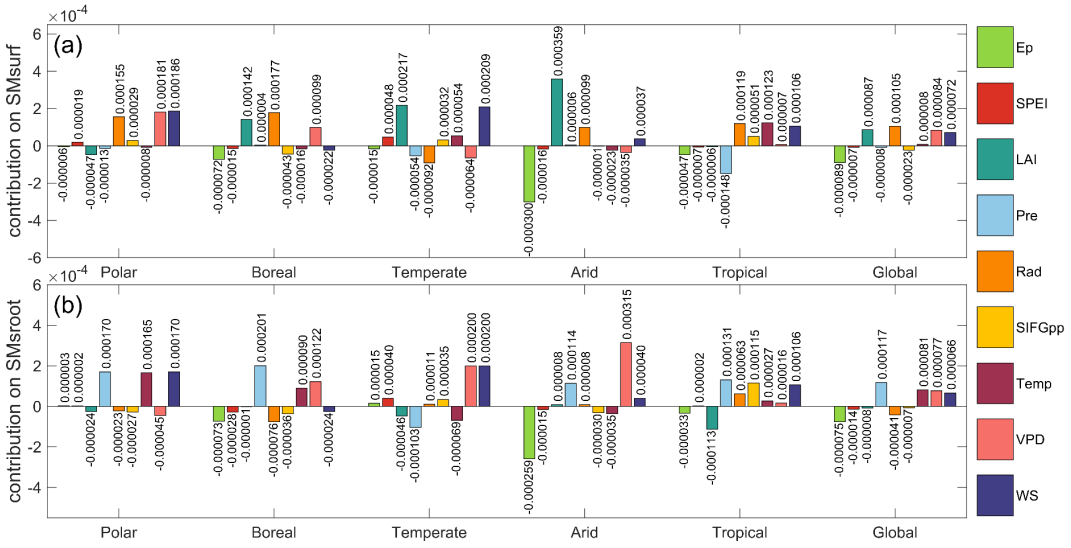

Figure. 3. Absolute contribution of vegetation to (a) SMsurf and (b) SMroot in different Köppen-Geiger climatic zones.

Figure.4 revealed the spatial distribution of the dominant factors influencing SM globally and statistically analyzed the dominant areas of each factor based on climatic zones. LAI and SIFGpp dominated the changes in SM over relatively small areas, but held a prominent position in typical vegetation restoration areas, such as the Loess Plateau in China. Regions predominantly influenced by SPEI were most concentrated around the Arabian Plateau. The dominant area of Pre was relatively large, mainly distributed in the South American highlands, the eastern coastal highland mountainous regions of North America, the Gedan Plateau, the East European Plain, the Pacific coast, and some desert areas in Australia. The distribution of dominant areas influenced by Ep was more scattered, primarily concentrated in the Arid region. From the high-latitude Polar region to the low-latitude Tropical, the area dominated by VPD gradually increased, overall dominating nearly a quarter of the global area. Temp and Rad had a relatively small proportion of domination globally, but held a larger proportion in the Polar region. WS occupied a dominant position in the variation of SM in the Polar and Boreal regions, with the dominant area decreasing gradually from high latitudes to low latitudes.

https://doi.org/10.5194/egusphere-2025-2828
Preprint. Discussion started: 8 July 2025
© Author(s) 2025. CC BY 4.0 License.

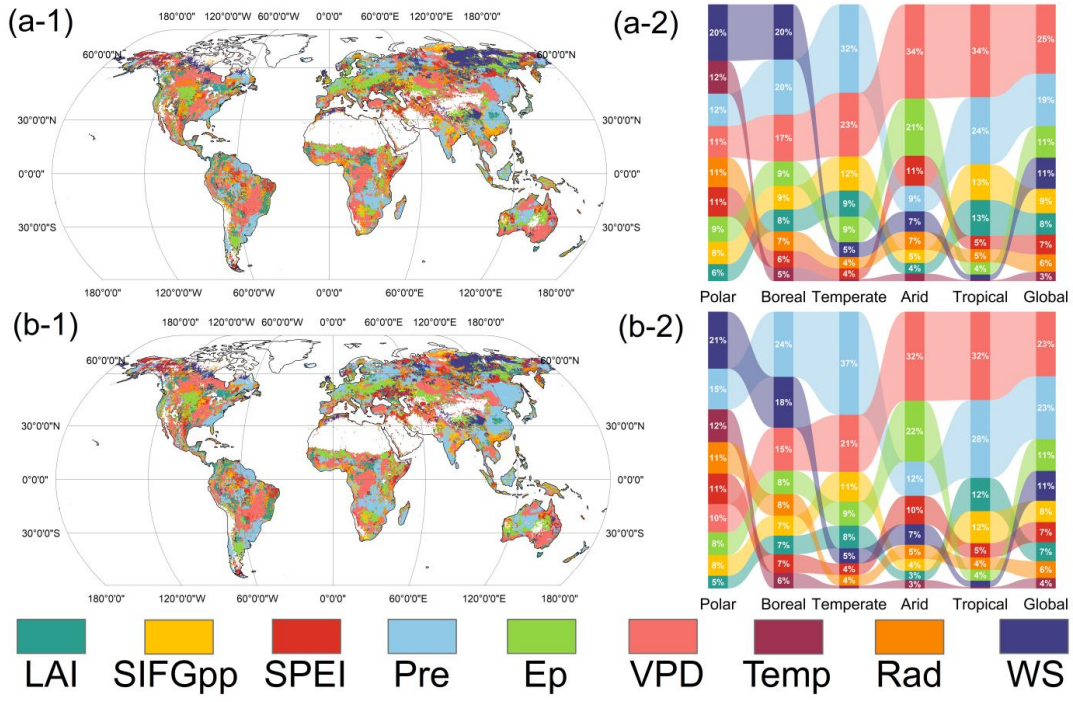

Figure. 4. (1) Spatial distribution and (2) proportion of dominant factors in different Köppen-Geiger climatic zones of (a) SMsurf and (b) SMroot.

3.3. Influencing pathways of vegetation indicators, drought indicator and climate factors on SM variations

The PLS-SEM model was constructed from both global and local perspectives, and the model's fit metrics were satisfactory. Specifically, the Goodness of Fit Index (GFI) was over 0.9, Root Mean Square Error of Approximation (RMSEA) was below 0.10, Comparative Fit Index (CFI) exceeded 0.9, Normed Fit Index (NFI) was above 0.9, Non-Normed Fit Index (NNFI) surpassed 0.9, and a $\chi 2/df$ ratio was less than 3 (Henseler and Sarstedt, 2013).

This study not only revealed the impact pathways of all driving factors on SM but also analyzed from a systemic perspective. Based on the functional correlations among factors, LAI and SIFGpp were classified as the ‘Global Greening’ module, while Pre, Ep, VPD, Temp, Rad, and WS were categorized as the ‘Climate Change’ module, with SPEI representing the ‘Drought Intensification’ module (Figure. 5). The paths we built not only included connections from ‘Global Greening,’ ‘Climate Change,’ and ‘Drought Intensification’ to SM, but also encompassed links from ‘Climate Change’ and ‘Drought Intensification’ to ‘Global Greening,’ as well as from ‘Climate Change’ to ‘Drought Intensification’. Regardless of whether viewed from climatic zones or globally, ‘Climate Change’ significantly moderated the impact of ‘Global Greening.’ In the high-latitude Polar region and Boreal region, the effects of each module on SM were not significant. In the Temperate region,

https://doi.org/10.5194/egusphere-2025-2828
Preprint. Discussion started: 8 July 2025
© Author(s) 2025. CC BY 4.0 License.

‘Climate Change’ exhibited a significant negative impact on SM ($p < 0.05$), while both ‘Global Greening’ and ‘Drought Intensification’ showed highly significant positive effects on SM ($p < 0.01$). In the Arid region, apart from the significant negative effect of ‘Global Greening’ on ‘Drought Intensification’ ($p < 0.05$), all three modules demonstrated highly significant direct positive effects on SM ($p < 0.01$). In the Tropical, the path coefficient of 'Global Greening' on SMsurf was 0.324 ($p < 0.05$), while its effect on SMroot was not significant. Additionally, 'Drought Intensification' exhibited a highly significant positive impact on SM ($p < 0.01$).

To further explore the pathways of various factors on SM, only LAI and SIFGpp were grouped as "Vegetation," while the remaining factors were not merged (Figure.5). The direct, indirect, and total path coefficients of various factors on SM were presented in Table S2 and Table S3. Only complete paths with all sub-paths being significant are focused on ($p < 0.05$). In the Polar region, all pathways were not significant, indicating a relatively simple or small impact on SM. In the Boreal region, Vegetation acted as the main mediating variable, with a total effect of 0.035 for Pre→Vegetation→SMsurf/SMroot, 0.087 for Temp → Vegetation → SMsurf/SMroot, and 0.270 for Rad→Temp→SMsurf/SMroot. The direct effect of Pre on SMroot was -0.362. In the Temperate region, the total effects were highest for Temp→Vegetation→SMsurf/SMroot, with values of 0.692 and 0.733 respectively. The total effects of Ep→SPEI→SMsurf/SMroot were 0.340 and 0.296 respectively. Temp acted as the mediating variable for WS and Rad's influence on SM. In the Arid region, the pathways were more complex, with Ep and Pre significantly impacting SM through SPEI, including Ep/Pre→SPEI→SMsurf/SMroot and Ep/Pre→SPEI→Vegetation→SMsurf/SMroot. Pre and Temp indirectly influenced SM through their positive effects on Vegetation. The total effects of Rad→Temp→SMsurf/SMroot were 0.583 and 0.618 respectively. In the Tropical, significant pathways included Rad→Temp→Vegetation→SMsurf/SMroot, Pre→SMsurf/SMroot, and SPEI→SMsurf/SMroot. From a global perspective, only the Rad→Temp→SMsurf/SMroot pathway was significant.

https://doi.org/10.5194/egusphere-2025-2828
Preprint. Discussion started: 8 July 2025
© Author(s) 2025. CC BY 4.0 License.

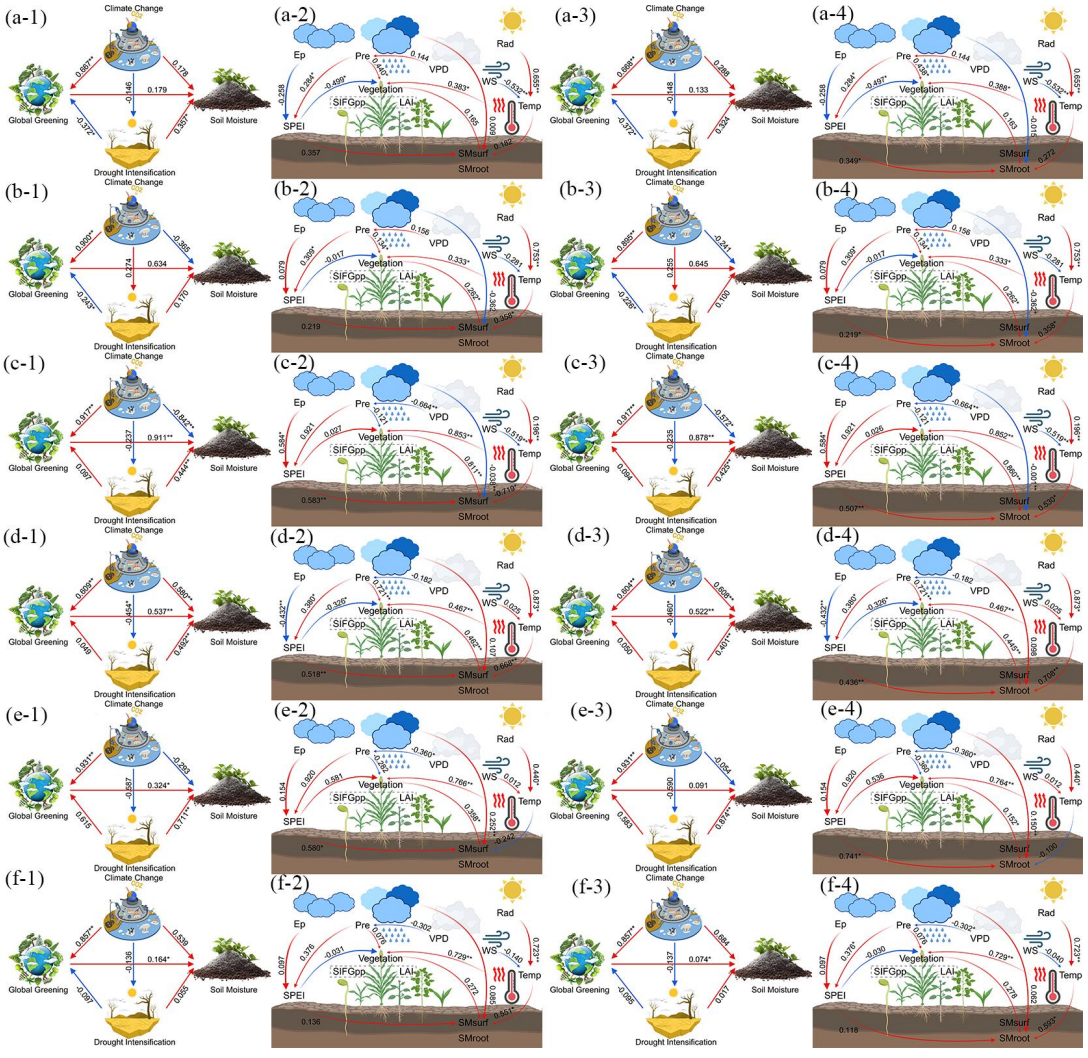

Figure. 5. The direct and indirect influences of driving factors on SMsurf and SMroot. (a), (b), (c), (d), (e), and (f) correspond to the Polar, Boreal, Temperate, Arid, Tropical, and Global regions, respectively. The first and third columns represent the impact pathways of different systems on SMsurf, while the second and fourth columns depict the influence pathways of all driving factors on SMroot. *, ** indicate the significance at $p < 0.05$, $p < 0.01$ levels, respectively.

3.4. The probability of SM loss under different stress scenarios

The probability of varying degrees of SM deficit under different stress scenarios was quantified using the optimized copula function, enabling the identification of high-risk factors affecting SM as well as high-risk sensitivity regions for SM depletion (Figure.S19, Figure. S20, Figure. S21). Taking the joint conditional probability of extreme soil moisture deficit under

https://doi.org/10.5194/egusphere-2025-2828
Preprint. Discussion started: 8 July 2025
© Author(s) 2025. CC BY 4.0 License.

extreme development scenarios as an example, we demonstrate the spatial distribution of high-risk areas for soil moisture deficit (Figure 6). From a spatial distribution perspective, areas with high sensitivity of SM to LAI and SIFGpp were concentrated in the Great Plains of North America, the Brown Coop, the Pampas grasslands, the Kalahari Basin, the East African Plateau, the Mediterranean region, the Australian Great Basin, as well as high plateau regions represented by the Iranian Plateau, the Deccan Plateau, the Mongolian Plateau, and the plains south of the Siberian Plateau. When LAI and SIFGpp were in an extreme development scenario, the probability of extreme SM deficit occurring was 0.08, while the probabilities of severe SM deficit were 0.23 and 0.22, respectively, and the probability of moderate SM deficit was both 0.34, indicating a high level of sensitivity in each scenario. It was observed that in any developmental scenario, the sensitivity of SM to Pre was higher in the Temperate, Arid, and Tropical regions located at mid to low latitudes, with values of 0.35, 0.34, and 0.33, respectively, whereas it was lower in the Polar and Boreal regions at high latitudes, with values of 0.3 and 0.31, respectively. Apart from the Eastern European Plain, the Congo Basin, and higher latitude regions, SM exhibited relatively high sensitivity to SPEI. The sensitivity of SM to Ep, VPD, Temp, Rad, and WS displayed distinct regional differences. Among them, the spatial distribution pattern of high sensitivity areas of SM to Ep, VPD, Temp, and Rad was similar, with high sensitivity areas concentrated in the Sahara Desert, the Arabian Plateau, the Rub' al Khali Desert, the lower reaches of the Indus River with the Taklimakan Desert in China, the Qinghai-Tibet Plateau, the Mongolian Plateau, the Labrador Plateau, and other highland and desert regions. Among these four factors, the high-value areas of SM sensitivity to Temp were more widely distributed compared to other factors. High-value areas of SM sensitivity to WS were detected in the Arabian Plateau, the Tarim Desert, and the Western Siberian Plain. In terms of climatic zones, overall, SM exhibited the greatest sensitivity to various factors in the Arid region, followed by the Temperate and Tropical regions. It was also evident that in the Arid region, the sensitivity of SM to Pre ranked fourth, while in any other climatic zone, Pre and SPEI were the most sensitive factors (Figure.7).

https://doi.org/10.5194/egusphere-2025-2828
Preprint. Discussion started: 8 July 2025
© Author(s) 2025. CC BY 4.0 License.

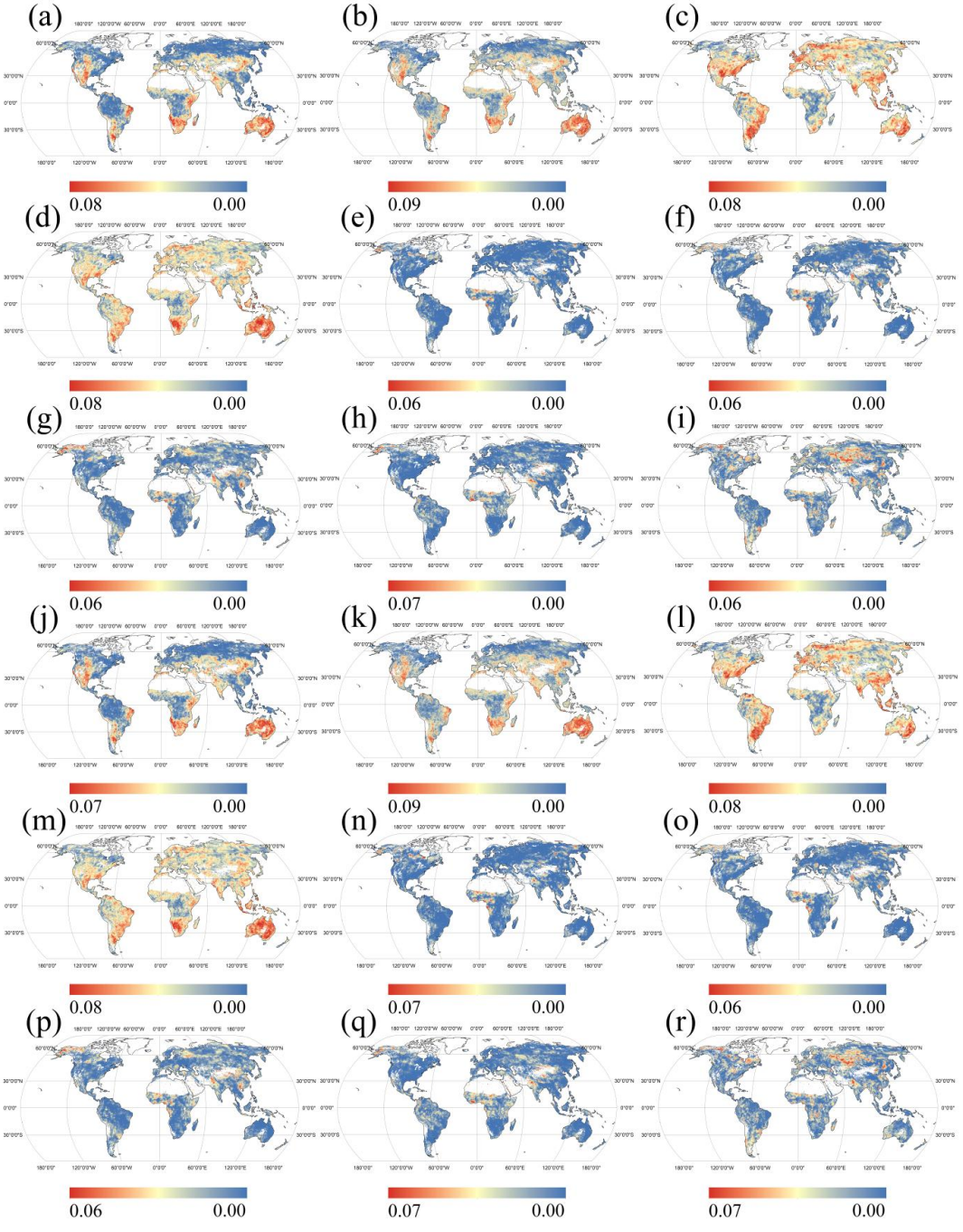

Figure 6. Spatial distribution of the joint conditional probability of extreme soil moisture deficit under extreme development scenarios. (a)-(i) represent the joint conditional probabilities of LAI, SIFGpp, SPEI, Pre, Ep, VPD, Temp, Rad, and WS with

https://doi.org/10.5194/egusphere-2025-2828
Preprint. Discussion started: 8 July 2025
© Author(s) 2025. CC BY 4.0 License.

SMsurf, respectively, and (j)-(r) represent the joint conditional probabilities of LAI, SIFGpp, SPEI, Pre, Ep, VPD, Temp, Rad, and WS with SMroot, respectively.

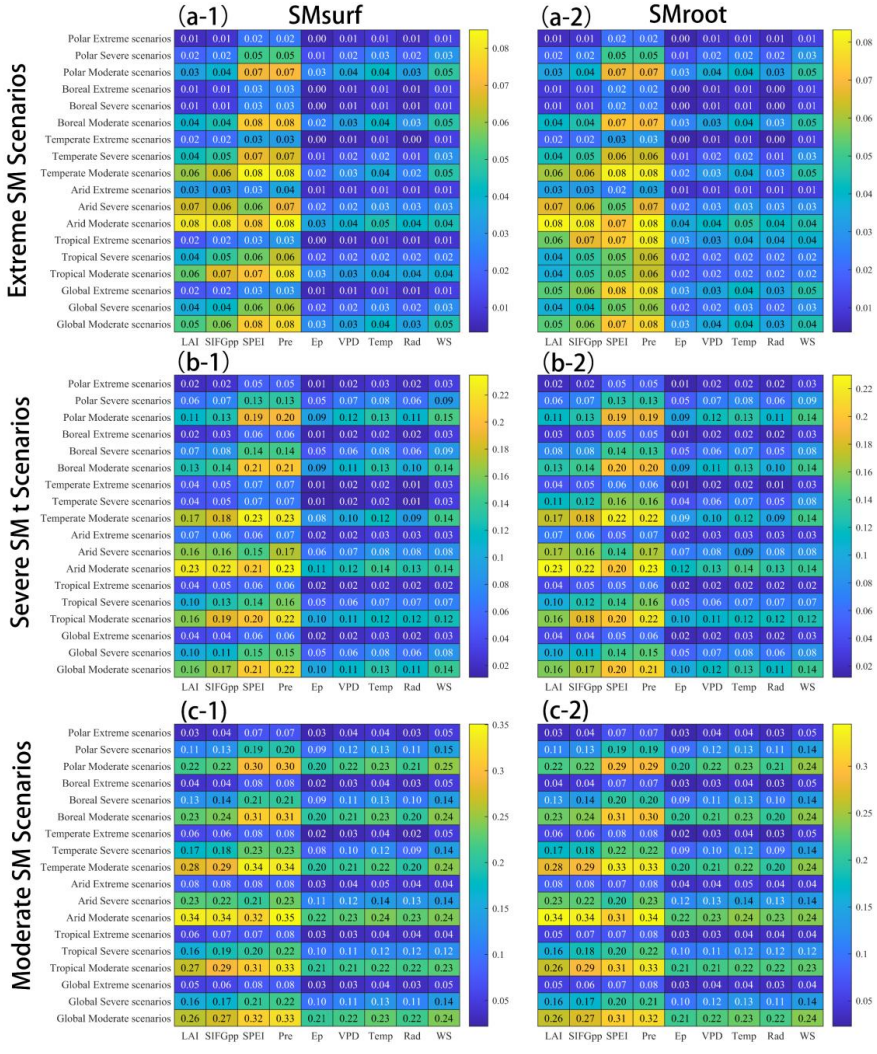

Figure. 7. The sensitivity of (1) SMsurf and (2) SMroot across various climatic zones under (a) Extreme, (b) Severe, and (c) Moderate development scenarios.

4. Discussion

4.1 Global Changes Jointly Impact SM

The hotspot regions of SM variation all exhibited fluctuating trends. However, a closer examination revealed that the fluctuation periods and frequencies of SM differed across regions (Figure. 1). For instance, Central and Eastern Europe, as

https://doi.org/10.5194/egusphere-2025-2828
Preprint. Discussion started: 8 July 2025
© Author(s) 2025. CC BY 4.0 License.

well as Central East Asia, both showed an accelerating drying trend during the growing season, likely due to increased water consumption by vegetation resulting from climate warming. Different regions, due to varying land use and conservation measures, also displayed distinct temporal evolution patterns. For example, in East Asia, the implementation of the Three-North Shelterbelt Program significantly enhanced the water conservation capacity of the root zone(Xu et al., 2023). In contrast, in Central and Eastern Europe, ongoing grassland shrinkage and simultaneous forest expansion led to an upward trend in SM depletion. In the southeastern region of the Great Artesian Basin, an increasing trend in SM was observed, likely due to the excessively high groundwater salinity in the basin, which precludes its direct use for irrigation. Consequently, artificial irrigation has replenished the consumption of SM.

Our study indicated that vegetation greening is one of the key factors contributing to the increase in global SMsurf, a viewpoint supported by related research. On the one hand, vegetation greening leads to an increase in vegetation cover, resulting in reduced soil evaporation (Li et al., 2019). Furthermore, vegetation greening results in the formation of a thicker litter layer, more extensive root systems, and increased organic matter, which aid in the formation of good soil aggregates, thereby enhancing the soil's water retention capacity (Yang et al., 2016; Yang et al., 2017; Zhang et al., 2019b; Adams et al., 1991). Simultaneously, we observed that vegetation greening led to a decrease in global SMroot, particularly in Tropical, possibly due to the dense vegetation characteristic of this climatic zone. Vegetation in Tropical rainforest areas is tall, with well-developed root systems anchored deep in the soil, leading to higher consumption of SMroot. Similarly, the vegetation index SIFGpp slightly decreased global SM due to increased productivity consuming more soil water. However, in the Temperate and Tropical regions, SIFGpp increased SMroot. This is probably because during high-temperature droughts, plants close leaf stomata to prevent water loss via transpiration; the resulting retained water may reduce vegetation greenness and leaf size (i.e., LAI) but can still maintain stable vegetation productivity (Novick et al., 2016; Oren et al., 1999; Sinclair et al., 2017). In other words, it is possible for SIFGpp to increase without an increase in vegetation transpiration water consumption in some high-temperature or drought-prone areas.

Several regional-scale studies have suggested that climate-induced vegetation changes increased evapotranspiration, resulting in drier soils (Deng et al., 2020b; Zeng et al., 2018). Our study found that at a global scale, SM increased concurrently with vegetation greening and enhanced productivity. The results from the PLS-SEM indicated that LAI and SIFGpp typically acted as intermediary variables transmitting the indirect effects of climate factors on SM, thereby demonstrating the viewpoint that the positive or negative impact of vegetation greening on SM largely depended on climatic conditions (Xu et al., 2023). Pre, as the primary water supply for SM, directly influenced its variability. Additionally, Pre was beneficial for vegetation greening and enhanced productivity. The restoration of grasslands and sparse vegetation contributed primarily to vegetation greening. Grassland root systems are shallow with low water absorption capacity, leading to greater retention of Pre in the soil,

https://doi.org/10.5194/egusphere-2025-2828
Preprint. Discussion started: 8 July 2025
© Author(s) 2025. CC BY 4.0 License.

further increasing SM (Wang et al., 2021). However, the contribution of Pre to the annual variation of SM was not significant due to the increasing decomposition of terrestrial Pre into evapotranspiration with rising temperatures (Pascolini-Campbell et al., 2021).

Our study also found that Ep was a significant factor contributing to global soil aridity, particularly pronounced in water-deficient Arid regions. The increase in Ep indicates an enhanced potential for evapotranspiration. In the Arid region where water resources are scarce and vegetation and crops have high water demands, the rise in Ep signifies greater water consumption by vegetation and soil evaporation, further exacerbating the decrease in SM (Condon et al., 2020; Feng et al., 2020). This may underscore the impact of water output on SM (Ge et al., 2020; Isabelle et al., 2020). Luo et al. (2023) indicated that the variations in global SMroot were primarily caused by Temp increases, with similar findings only observed in Tropical. This is attributed to the higher Temp in the Tropical, where climate warming and high Temp lead to increased evaporation demand and atmospheric dryness (Cheng and Huang, 2016; Deng et al., 2020a; Fang et al., 2022). VPD played a dominant role in the changes in local SM, but its positive and negative contributions offset each other at a global scale. We found a more significant impact of VPD on SM reduction in regions with high VPD values globally, particularly in the Arid and Temperate regions, due to higher VPD leading to increased land evapotranspiration, further accelerating SM depletion (Luo et al., 2023), consistent with the conclusions of Qing et al. (2023).We also found that WS played a dominant role in the changes of SM in high latitude regions in the Northern Hemisphere, primarily resulting in SM reduction. This was further validated through PLS-SEM, where higher WS accelerated the rate of water evaporation from both the soil (direct effect) and vegetation surfaces (indirect effect) into the atmosphere, consequently exacerbating SM loss (Tang and Tang, 2021; Shi et al., 2022; Roderick et al., 2007; Zhang et al., 2007).

Global atmospheric circulation can impact regional water cycles (Allen and Ingram, 2002). Therefore, this study examined the teleconnection relationship between global environmental factors and SM through wavelet coherence analysis (Figure. S17 and Figure. S18). he cone-shaped thin lines in the Figureures denoted the effective spectral region, with thick lines within the effective area representing the 95% confidence interval of significant signals; arrows indicate phase differences, leftward implying a negative correlation between two sequences, while rightward indicating a positive correlation. All four global environmental factors exhibited significant cycles of 8-16 months at both global and climatic zones scales. Additionally, NAO, PDO, and AO showed multiple significant cycles of 4-8 months in Polar, Boreal, and Arid. In the Tropical, NAO and PDO were negatively or approximately negatively correlated with SM, while in other climatic zones, they demonstrated positive or nearly positive correlations. The high-energy areas in the Arid and Polar regions were relatively scattered, with NAO exerting the most significant impact on SM and ENSO showing the least influence. In the Boreal, Temperate, and Tropical regions, the high-energy zones were more continuous, with resonance periods concentrated around 2001-2008, 2010-

https://doi.org/10.5194/egusphere-2025-2828
Preprint. Discussion started: 8 July 2025
© Author(s) 2025. CC BY 4.0 License.

2018, and 2019-2020, with only 2-3 years of insignificant correlation. Overall, the correlation between ENSO and SM was relatively weak, and the NAO and PDO had the greatest influence on SM. Meanwhile, it is important to note that global environmental factors mostly indirectly affect hydrological processes by disturbing regional climates and vegetation (Li et al., 2021b; Su et al., 2019; Huang et al., 2013; Yang et al., 2021).

4.2 High-risk factors for SM loss

For the first time, we calculated the probability of SM loss under different stress scenarios. The results indicated that Pre and SPEI had the highest probabilities of causing SM loss. In all climatic zones, precipitation deficit was consistently the highest risk factor for SM depletion. As the primary source of SM, Pre plays a crucial role in maintaining the dynamic balance of SM (Chen et al., 2019; Maina et al., 2022). Insufficient precipitation disrupts this balance, leading to soil drying and adversely affecting both vegetation and SM (Lesk et al., 2021). In arid regions, the probability of vegetation-induced SM loss was second only to Pre, and, apart from arid zones, the SM deficit probabilities in other climatic regions were also significantly influenced by SPEI.

However, why does Ep contribute the most to SM deficit, while Pre and SPEI cause the highest probability of SM loss? This may seem confusing. We believe the results are not contradictory. The numerical simulations based on RF quantify the average predictive contribution of variables to SM, reflecting the dominant role of precipitation deficits and SPEI in the overall data. On the other hand, the Copula method, through joint probability distributions, reveals the extreme dependence relationships between variables, indicating that under extreme conditions, such as drought, the synergistic effect of precipitation deficit and SPEI significantly amplifies the conditional probability of SM loss. Machine learning focuses on the "importance of variables under typical scenarios," while Copula emphasizes the "risk coupling under extreme conditions." For example, SPEI may be weakened in contribution within machine learning models due to its inclusion of precipitation data, but the Copula method captures its tail dependence with precipitation during droughts, explaining the extreme risk triggered by their combined effects. Therefore, these two approaches, from the perspectives of predictive modeling and risk probability, complement each other and jointly help us understand the evolving patterns of SM.

4.3. Implications for Sustainable Water Resource Management

SM ranks among crucial indicators for agricultural drought. It has a direct impact on soil physical and chemical characteristics as well as vegetation development, thereby exerting a substantial influence on global food production (Liu and Yang, 2023). Liu et al. (2023) has found a downward trend from 1980 to 2000, followed by a gradual increase after 2000. The serious consequences of soil drought have been recognized, leading to the implementation of multiple tree - planting initiatives aimed at averting land deterioration and desert encroachment, such as the Great Green Wall in the Sahara and Sahel regions

https://doi.org/10.5194/egusphere-2025-2828
Preprint. Discussion started: 8 July 2025
© Author(s) 2025. CC BY 4.0 License.

(Goffner et al., 2019), the Indian banyan hedge (Mladenova et al., 2019), and the Three-North Shelterbelt Program (Qiu et al., 2017), which have substantially transformed the vegetation conFigureurations in relevant semi - arid or arid zones, and in doing so, accomplished the preservation of water resources. Additionally, beneficial climate shifts from arid to humid can promote vegetation proliferation, thereby serving the goal of safeguarding SM, but the reduction in SM triggered by the expansion of vegetation resulting from warming might give rise to severe drought (Qiu et al., 2021; Zhang et al., 2021). In other words, despite the continuous increase in SM since 2000, many regions still harbor potential ecological drought risks within the trends of climate change and greening (Holl and Brancalion, 2020; Liu et al., 2020a). In these areas, the cultivation of drought-resistant vegetation indeed plays an important role in soil and water conservation and sand fixation. However, considering the possible scarcity of water resources in these regions, a careful and strict assessment of the water requirements of vegetation and planting density/structure is needed before implementation to promote ecological sustainable development (Strassburg et al., 2020; Qiu et al., 2021).

4.4. Limitations, Uncertainties, and Prospects

While our study attempted to reveal the reasons for SM variability using a more comprehensive set of factors and analyzed the influencing pathways, thus filling the knowledge gap on long-term SM at different depths globally, there were still some limitations and uncertainties. Firstly, factors closely related to SM dynamics such as atmospheric circulation (Liang et al., 2023), snowmelt (Bales et al., 2011), and water diversion projects (Liu and Zheng, 2002) may require further exploration. However, quantifying the impact of some of these factors on SM could prove challenging. Additionally, the response mechanisms of regional agricultural irrigation and groundwater extraction to SM need further investigation (Zhang et al., 2019a). Finally, this study calculated the probability of SM deficit by considering only the individual effects of specific factors under particular scenarios, without accounting for the synergistic and compound impacts of factors such as temperature and precipitation on SM. Therefore, further analysis of the probability of SM deficit using high-dimensional copula could be a potential direction for future research.

5. Conclusion

This study analyzed the spatiotemporal evolution characteristics of global SMsurf and SMroot from 2001 to 2021. By employing a comprehensive set of factors, the study aimed to reveal the contribution and pathways (direct and indirect) of vegetation characteristics, climate factors, and drought indices to SM variability. Furthermore, it ultimately revealing the probability of SM deficit under different stress scenarios.

(1) The SM variation trends exhibited a significant regional convergence and spatial differentiation pattern.

https://doi.org/10.5194/egusphere-2025-2828
Preprint. Discussion started: 8 July 2025
© Author(s) 2025. CC BY 4.0 License.

(2) The increase in surface and root-zone SM globally can be attributed to vegetation greening and precipitation, respectively. And Atmospheric water demand (Ep) was identified as the primary cause of global SM aridity.

(3) Vegetation typically acted as an intermediate variable transmitting the indirect effects of climate factors and global environmental factors on SM.

(4) Precipitation, the standardized precipitation-evapotranspiration index, and vegetation dynamics were the primary factors driving the highest probability of SM deficit.

The research findings are expected to provide decision-making support for global sustainable water resource management under climate change conditions.

Author Contribution declaration

Conceptualization and supervision: Z.W., W.Z, and Y.L.; Design and methodology: Z.W., Z.Z. and R.W.; Data analysis: Z.W., R.W., and Y.Z.; Data curation: N.Z., Z.W. and Y.L.; Writing-original draft preparation: Z.W. and Y.L.; Writing-review and editing: C.C. and Y.L..

Declaration of Competing Interest

The authors declare that they have no known competing financial interests or personal relationships that could have appeared to influence the work reported in this paper.

Funding

This work was supported by National Natural Science Foundation of China (No. 42477522, No. U1203182, No. 51279166); the Key R&D Plan of Shaanxi Province (No. 2024SF-YBXM-621); supported by a grant from State Key Laboratory of Resources and Environmental Information System; the “Open Research Fund of Key Laboratory of Digital Earth Science, Chinese Academy of Sciences” (No. 2022LDE003).

Acknowledgments

We acknowledge for the data support from ‘Loess plateau science data center, National Earth System Science Data Sharing Infrastructure, National Science & Technology Infrastructure of China, National Tibetan Plateau Scientific Data Center’.

Reference

Adams, P. W., Flint, A. L., and Fredriksen, R. L.: Long-term patterns in soil moisture and revegetation after a clearcut of a Douglas-fir forest in Oregon, Forest Ecology and Management, 41, 249-263, https://doi.org/10.1016/0378-1127(91)90107-7, 1991.

Allen, M. R. and Ingram, W. J.: Constraints on future changes in climate and the hydrologic cycle, Nature, 419, 224-+, 10.1038/nature01092, 2002.

https://doi.org/10.5194/egusphere-2025-2828
Preprint. Discussion started: 8 July 2025
© Author(s) 2025. CC BY 4.0 License.

586 Aragao, L.: ENVIRONMENTAL SCIENCE The rainforest's water pump, Nature, 489, 217-218,
587 10.1038/nature11485, 2012.
588 Bales, R. C., Hopmans, J. W., O'Geen, A. T., Meadows, M., Hartsough, P. C., Kirchner, P., Hunsaker, C. T., and
589 Beaudette, D.: Soil Moisture Response to Snowmelt and Rainfall in a Sierra Nevada Mixed-Conifer Forest, Vadose
590 Zone Journal, 10, 786-799, 10.2136/vzj2011.0001, 2011.
591 Beck, H. E., Zimmermann, N. E., McVicar, T. R., Vergopolan, N., Berg, A., and Wood, E. F.: Present and future
592 Koppen-Geiger climate classification maps at 1-km resolution, Scientific Data, 5, 10.1038/sdata.2018.214, 2018.
593 Beguería, S., Vicente-Serrano, S. M., Reig, F., and Latorre, B.: Standardized precipitation evapotranspiration index
594 (SPEI) revisited: parameter fitting, evapotranspiration models, tools, datasets and drought monitoring, International
595 Journal of Climatology, 34, 3001-3023, 10.1002/joc.3887, 2014.
596 Berdugo, M., Delgado-Baquerizo, M., Soliveres, S., Hernández-Clemente, R., Zhao, Y. C., Gaitan, J. J., Gross, N.,
597 Saiz, H., Maire, V., Lehman, A., Rillig, M. C., Solé, R. V., and Maestre, F. T.: Global ecosystem thresholds driven
598 by aridity, Science, 367, 787-+, 10.1126/science.aay5958, 2020.
599 Bonan, G. B.: Forests and climate change: Forcings, feedbacks, and the climate benefits of forests, Science, 320,
600 1444-1449, 10.1126/science.1155121, 2008.
601 Boulton, C. A., Lenton, T. M., and Boers, N.: Pronounced loss of Amazon rainforest resilience since the early
602 2000s, Nature Climate Change, 12, 271-278, 10.1038/s41558-022-01287-8, 2022.
603 Breiman, L.: Random Forests, Machine Learning, 45, 5-32, 10.1023/A:1010933404324, 2001.
604 Chang, Q. Q., He, H. L., Ren, X. L., Zhang, L., Feng, L. L., Lv, Y., Zhang, M. Y., Xu, Q., Liu, W. H., Zhang, Y.
605 H., and Wang, T. X.: Soil moisture drives the spatiotemporal patterns of asymmetry in vegetation productivity
606 responses across China, Science of the Total Environment, 855, 10.1016/j.scitotenv.2022.158819, 2023.
607 Chen, Y. Z., Feng, X., Fu, B., Shi, W. Y., Yin, L. C., and Lv, Y. H.: Recent Global Cropland Water Consumption
608 Constrained by Observations, Water Resources Research, 55, 3708-3738, 10.1029/2018wr023573, 2019.
609 Cheng, S., Guan, X., Huang, J., Ji, F., and Guo, R.: Long-term trend and variability of soil moisture over East Asia,
610 Journal of Geophysical Research: Atmospheres, 120, 8658-8670, https://doi.org/10.1002/2015JD023206, 2015.
611 Cheng, S. J. and Huang, J. P.: Enhanced soil moisture drying in transitional regions under a warming climate,
612 Journal of Geophysical Research-Atmospheres, 121, 2542-2555, 10.1002/2015jd024559, 2016.
613 Cho, E. and Choi, M.: Regional scale spatio-temporal variability of soil moisture and its relationship with
614 meteorological factors over the Korean peninsula, Journal of Hydrology, 516, 317-329,
615 10.1016/j.jhydrol.2013.12.053, 2014.
616 Clewley, D., Whitcomb, J. B., Akbar, R., Silva, A. R., Berg, A., Adams, J. R., Caldwell, T., Entekhabi, D., and
617 Moghaddam, M.: A Method for Upscaling In Situ Soil Moisture Measurements to Satellite Footprint Scale Using
618 Random Forests, IEEE Journal of Selected Topics in Applied Earth Observations and Remote Sensing, 10, 2663-
619 2673, 10.1109/JSTARS.2017.2690220, 2017.
620 Condon, L. E., Atchley, A. L., and Maxwell, R. M.: Evapotranspiration depletes groundwater under warming over
621 the contiguous United States, Nature Communications, 11, 873, 10.1038/s41467-020-14688-0, 2020.
622 Deng, Y., Wang, S., Bai, X., Luo, G., Wu, L., Cao, Y., Li, H., Li, C., Yang, Y., Hu, Z., and Tian, S.: Variation
623 trend of global soil moisture and its cause analysis, Ecological Indicators, 110, 105939,
624 https://doi.org/10.1016/j.ecolind.2019.105939, 2020a.
625 Deng, Y., Wang, S., Bai, X., Luo, G., Wu, L., Chen, F., Wang, J., Li, C., Yang, Y., Hu, Z., Tian, S., and Lu, Q.:
626 Vegetation greening intensified soil drying in some semi-arid and arid areas of the world, Agricultural and Forest
627 Meteorology, 292-293, 108103, https://doi.org/10.1016/j.agrformet.2020.108103, 2020b.
628 Dorigo, W., de Jeu, R., Chung, D., Parinussa, R., Liu, Y., Wagner, W., and Fernández-Prieto, D.: Evaluating global
629 trends (1988-2010) in harmonized multi-satellite surface soil moisture, Geophysical Research Letters, 39,
630 10.1029/2012gl052988, 2012.

https://doi.org/10.5194/egusphere-2025-2828
Preprint. Discussion started: 8 July 2025
© Author(s) 2025. CC BY 4.0 License.

631 Dorigo, W., Wagner, W., Albergel, C., Albrecht, F., Balsamo, G., Brocca, L., Chung, D., Ertl, M., Forkel, M.,
632 Gruber, A., Haas, E., Hamer, P. D., Hirschi, M., Ikonen, J., de Jeu, R., Kidd, R., Lahoz, W., Liu, Y. Y., Miralles,
633 D., Mistelbauer, T., Nicolai-Shaw, N., Parinussa, R., Pratola, C., Reimer, C., van der Schalie, R., Seneviratne, S.
634 I., Smolander, T., and Lecomte, P.: ESA CCI Soil Moisture for improved Earth system understanding: State-of-the
635 art and future directions, Remote Sensing of Environment, 203, 185-215, https://doi.org/10.1016/j.rse.2017.07.001,
636 2017.
637 Duan, L., Huang, M., and Zhang, L.: Use of a state-space approach to predict soil water storage at the hillslope
638 scale on the Loess Plateau, China, CATENA, 137, 563-571, https://doi.org/10.1016/j.catena.2015.11.003, 2016.
639 Fang, Z. X., Zhang, W. M., Brandt, M., Abdi, A. M., and Fensholt, R.: Globally Increasing Atmospheric Aridity
640 Over the 21st Century, Earths Future, 10, 10.1029/2022ef003019, 2022.
641 Feng, H.: Individual contributions of climate and vegetation change to soil moisture trends across multiple spatial
642 scales, Scientific Reports, 6, 32782, 10.1038/srep32782, 2016.
643 Feng, H. H. and Zhang, M. Y.: Global land moisture trends: drier in dry and wetter in wet over land, Scientific
644 Reports, 5, 10.1038/srep18018, 2015.
645 Feng, S., Liu, J., Zhang, Q., Zhang, Y., Singh, V. P., Gu, X., and Sun, P.: A global quantitation of factors affecting
646 evapotranspiration variability, Journal of Hydrology, 584, 124688, https://doi.org/10.1016/j.jhydrol.2020.124688,
647 2020.
648 Ge, J., Pitman, A. J., Guo, W., Zan, B., and Fu, C.: Impact of revegetation of the Loess Plateau of China on the
649 regional growing season water balance, Hydrol. Earth Syst. Sci., 24, 515-533, 10.5194/hess-24-515-2020, 2020.
650 Genest, C. and Favre, A.-C.: Everything You Always Wanted to Know about Copula Modeling but Were Afraid
651 to Ask, Journal of Hydrologic Engineering, 12, 347-368, 2007.
652 Gocic, M. and Trajkovic, S.: Analysis of changes in meteorological variables using Mann-Kendall and Sen's slope
653 estimator statistical tests in Serbia, Global and Planetary Change, 100, 172-182,
654 https://doi.org/10.1016/j.gloplacha.2012.10.014, 2013.
655 Goffner, D., Sinare, H., and Gordon, L. J.: The Great Green Wall for the Sahara and the Sahel Initiative as an
656 opportunity to enhance resilience in Sahelian landscapes and livelihoods, Regional Environmental Change, 19,
657 1417-1428, 10.1007/s10113-019-01481-z, 2019.
658 Green, J. K., Seneviratne, S. I., Berg, A. M., Findell, K. L., Hagemann, S., Lawrence, D. M., and Gentine, P.: Large
659 influence of soil moisture on long-term terrestrial carbon uptake, Nature, 565, 476-479, 10.1038/s41586-018-0848-
660 x, 2019.
661 Gruber, A., Scanlon, T., van der Schalie, R., Wagner, W., and Dorigo, W.: Evolution of the ESA CCI Soil Moisture
662 climate data records and their underlying merging methodology, Earth Syst. Sci. Data, 11, 717-739, 10.5194/essd-
663 11-717-2019, 2019.
664 Guan, Y., Gu, X., Slater, L. J., Li, J., Kong, D., and Zhang, X.: Spatio-temporal variations in global surface soil
665 moisture based on multiple datasets: Intercomparison and climate drivers, Journal of Hydrology, 625, 130095,
666 https://doi.org/10.1016/j.jhydrol.2023.130095, 2023.
667 Hair, J. F., Hult, G. T. M., Ringle, C., and Sarstedt, M.: A Primer on Partial Least Squares Structural Equation
668 Modeling (PLS-SEM), SAGE Publications2016.
669 Henseler, J. and Sarstedt, M.: Goodness-of-fit indices for partial least squares path modeling, Computational
670 Statistics, 28, 565-580, 10.1007/s00180-012-0317-1, 2013.
671 Hirschi, M., Mueller, B., Dorigo, W., and Seneviratne, S. I.: Using remotely sensed soil moisture for land–
672 atmosphere coupling diagnostics: The role of surface vs. root-zone soil moisture variability, Remote Sensing of
673 Environment, 154, 246-252, https://doi.org/10.1016/j.rse.2014.08.030, 2014a.

https://doi.org/10.5194/egusphere-2025-2828
Preprint. Discussion started: 8 July 2025
© Author(s) 2025. CC BY 4.0 License.

Hirschi, M., Mueller, B., Dorigo, W., and Seneviratne, S. I.: Using remotely sensed soil moisture for land-atmosphere coupling diagnostics: The role of surface vs. root-zone soil moisture variability, Remote Sensing of Environment, 154, 246-252, 10.1016/j.rse.2014.08.030, 2014b.

Holl, K. D. and Brancalion, P. H. S.: Tree planting is not a simple solution, Science, 368, 580-581, doi:10.1126/science.aba8232, 2020.

Hu, W. and Si, B. C.: Technical note: Multiple wavelet coherence for untangling scale-specific and localized multivariate relationships in geosciences, Hydrol. Earth Syst. Sci., 20, 3183-3191, 10.5194/hess-20-3183-2016, 2016.

Huang, W., Chen, F., Feng, S., Chen, J., and Zhang, X.: Interannual precipitation variations in the mid-latitude Asia and their association with large-scale atmospheric circulation, Chinese Science Bulletin, 58, 3962-3968, 10.1007/s11434-013-5970-4, 2013.

Huang, X., Shi, Z. H., Zhu, H. D., Zhang, H. Y., Ai, L., and Yin, W.: Soil moisture dynamics within soil profiles and associated environmental controls, CATENA, 136, 189-196, https://doi.org/10.1016/j.catena.2015.01.014, 2016.

Isabelle, P.-E., Nadeau, D. F., Anctil, F., Rousseau, A. N., Jutras, S., and Music, B.: Impacts of high precipitation on the energy and water budgets of a humid boreal forest, Agricultural and Forest Meteorology, 280, 107813, https://doi.org/10.1016/j.agrformet.2019.107813, 2020.

Jasechko, S., Sharp, Z. D., Gibson, J. J., Birks, S. J., Yi, Y., and Fawcett, P. J.: Terrestrial water fluxes dominated by transpiration, Nature, 496, 347-+, 10.1038/nature11983, 2013.

Jiao, W. Z., Wang, L. X., Smith, W. K., Chang, Q., Wang, H. L., and D'Odorico, P.: Observed increasing water constraint on vegetation growth over the last three decades, Nature Communications, 12, 10.1038/s41467-021-24016-9, 2021.

Jung, M., Reichstein, M., Ciais, P., Seneviratne, S. I., Sheffield, J., Goulden, M. L., Bonan, G., Cescatti, A., Chen, J., de Jeu, R., Dolman, A. J., Eugster, W., Gerten, D., Gianelle, D., Gobron, N., Heinke, J., Kimball, J., Law, B. E., Montagnani, L., Mu, Q., Mueller, B., Oleson, K., Papale, D., Richardson, A. D., Roupsard, O., Running, S., Tomelleri, E., Viovy, N., Weber, U., Williams, C., Wood, E., Zaehle, S., and Zhang, K.: Recent decline in the global land evapotranspiration trend due to limited moisture supply, Nature, 467, 951-954, 10.1038/nature09396, 2010a.

Jung, M., Reichstein, M., Ciais, P., Seneviratne, S. I., Sheffield, J., Goulden, M. L., Bonan, G., Cescatti, A., Chen, J. Q., de Jeu, R., Dolman, A. J., Eugster, W., Gerten, D., Gianelle, D., Gobron, N., Heinke, J., Kimball, J., Law, B. E., Montagnani, L., Mu, Q. Z., Mueller, B., Oleson, K., Papale, D., Richardson, A. D., Roupsard, O., Running, S., Tomelleri, E., Viovy, N., Weber, U., Williams, C., Wood, E., Zaehle, S., and Zhang, K.: Recent decline in the global land evapotranspiration trend due to limited moisture supply, Nature, 467, 951-954, 10.1038/nature09396, 2010b.

Legates, D. R., Mahmood, R., Levia, D. F., DeLiberty, T. L., Quiring, S. M., Houser, C., and Nelson, F. E.: Soil moisture: A central and unifying theme in physical geography, Progress in Physical Geography-Earth and Environment, 35, 65-86, 10.1177/0309133310386514, 2011.

Lesk, C., Coffel, E., Winter, J., Ray, D., Zscheischler, J., Seneviratne, S. I., and Horton, R.: Stronger temperature–moisture couplings exacerbate the impact of climate warming on global crop yields, Nature Food, 2, 683-691, 10.1038/s43016-021-00341-6, 2021.

Li, B., Yang, Y., and Li, Z.: Combined effects of multiple factors on spatiotemporally varied soil moisture in China's Loess Plateau, Agricultural Water Management, 258, 107180, https://doi.org/10.1016/j.agwat.2021.107180, 2021a.

Li, B. B., Yang, Y., and Li, Z.: Combined effects of multiple factors on spatiotemporally varied soil moisture in China's Loess Plateau, Agricultural Water Management, 258, 10.1016/j.agwat.2021.107180, 2021b.

https://doi.org/10.5194/egusphere-2025-2828
Preprint. Discussion started: 8 July 2025
© Author(s) 2025. CC BY 4.0 License.

Li, C. J., Fu, B. J., Wang, S., Stringer, L. C., Wang, Y. P., Li, Z. D., Liu, Y. X., and Zhou, W. X.: Drivers and impacts of changes in China's drylands, Nature Reviews Earth & Environment, 2, 858-873, 10.1038/s43017-021-00226-z, 2021c.

Li, J. and Xiao, Z. Q.: Evaluation of the version 5.0 global land surface satellite (GLASS) leaf area index product derived from MODIS data, International Journal of Remote Sensing, 41, 9140-9160, 10.1080/01431161.2020.1797222, 2020.

Li, W. T., Migliavacca, M., Forkel, M., Walther, S., Reichstein, M., and Orth, R.: Revisiting Global Vegetation Controls Using Multi-Layer Soil Moisture, Geophysical Research Letters, 48, 10.1029/2021gl092856, 2021d.

Li, X. and Xiao, J. F.: A Global, 0.05-Degree Product of Solar-Induced Chlorophyll Fluorescence Derived from OCO-2, MODIS, and Reanalysis Data, Remote Sensing, 11, 10.3390/rs11050517, 2019.

Li, X. Y., Zou, L., Xia, J., Dou, M., Li, H. W., and Song, Z. H.: Untangling the effects of climate change and land use/cover change on spatiotemporal variation of evapotranspiration over China, Journal of Hydrology, 612, 10.1016/j.jhydrol.2022.128189, 2022.

Li, X. Z., Xu, X. L., Liu, W., He, L., Xu, C. H., Zhang, R. F., Chen, L., and Wang, K. L.: Revealing the scale-specific influence of meteorological controls on soil water content in a karst depression using wavelet coherency, Agriculture Ecosystems & Environment, 279, 89-99, 10.1016/j.agee.2019.04.016, 2019.

Li, Y., Piao, S. L., Li, L. Z. X., Chen, A. P., Wang, X. H., Ciais, P., Huang, L., Lian, X., Peng, S. S., Zeng, Z. Z., Wang, K., and Zhou, L. M.: Divergent hydrological response to large-scale afforestation and vegetation greening in China, Science Advances, 4, 10.1126/sciadv.aar4182, 2018.

Lian, X., Piao, S. L., Li, L. Z. X., Li, Y., Huntingford, C., Ciais, P., Cescatti, A., Janssens, I. A., Penuelas, J., Buermann, W., Chen, A. P., Li, X. Y., Myneni, R. B., Wang, X. H., Wang, Y. L., Yang, Y. T., Zeng, Z. Z., Zhang, Y. Q., and McVicar, T. R.: Summer soil drying exacerbated by earlier spring greening of northern vegetation, Science Advances, 6, 10.1126/sciadv.aax0255, 2020.

Liang, J., Yong, Y., and Hawcroft, M. K.: Long-term trends in atmospheric rivers over East Asia, Climate Dynamics, 60, 643-666, 10.1007/s00382-022-06339-5, 2023.

Liu, C. and Zheng, H.: South-to-north Water Transfer Schemes for China, International Journal of Water Resources Development, 18, 453-471, 10.1080/0790062022000006934, 2002.

Liu, L., Gudmundsson, L., Hauser, M., Qin, D., Li, S., and Seneviratne, S.: Soil moisture dominates dryness stress on ecosystem production globally, Nat. Commun., 11, 4892, 2020a.

Liu, L. B., Gudmundsson, L., Hauser, M., Qin, D. H., Li, S. C., and Seneviratne, S. I.: Soil moisture dominates dryness stress on ecosystem production globally, Nature Communications, 11, 10.1038/s41467-020-18631-1, 2020b.

Liu, Y., Jing, W., Wang, Q., and Xia, X.: Generating high-resolution daily soil moisture by using spatial downscaling techniques: a comparison of six machine learning algorithms, Advances in Water Resources, 141, 103601, https://doi.org/10.1016/j.advwatres.2020.103601, 2020c.

Liu, Y. X., Yang, Y. P., and Song, J.: Variations in Global Soil Moisture During the Past Decades: Climate or Human Causes?, Water Resources Research, 59, 10.1029/2023wr034915, 2023.

Liu, Y. X. Y. and Yang, Y. P.: Spatial-temporal variability pattern of multi-depth soil moisture jointly driven by climatic and human factors in China, Journal of Hydrology, 619, 10.1016/j.jhydrol.2023.129313, 2023.

Luo, X. R., Li, S. D., Yang, W. N., Liu, L., Shi, Y. H., Lai, Y. S., Yu, P., Yang, Z. H., Luo, K., Zhou, T., Yang, X., Wang, X., Chen, S. H., and Tang, X. L.: Spatio-temporal changes in global root zone soil moisture from 1981 to 2017, Journal of Hydrology, 626, 10.1016/j.jhydrol.2023.130297, 2023.

Ma, W., Li, G., Wu, J., Xu, G., and Wu, J.: Response of soil labile organic carbon fractions and carbon-cycle enzyme activities to vegetation degradation in a wet meadow on the Qinghai–Tibet Plateau, Geoderma, 377, 114565, https://doi.org/10.1016/j.geoderma.2020.114565, 2020.

https://doi.org/10.5194/egusphere-2025-2828
Preprint. Discussion started: 8 July 2025
© Author(s) 2025. CC BY 4.0 License.

Maina, F. Z., Kumar, S. V., Albergel, C., and Mahanama, S. P.: Warming, increase in precipitation, and irrigation enhance greening in High Mountain Asia, Communications Earth & Environment, 3, 43, 10.1038/s43247-022-00374-0, 2022.

Martens, B., Miralles, D. G., Lievens, H., van der Schalie, R., de Jeu, R. A. M., Fernández-Prieto, D., Beck, H. E., Dorigo, W. A., and Verhoest, N. E. C.: GLEAM v3: satellite-based land evaporation and root-zone soil moisture, Geoscientific Model Development, 10, 1903-1925, 10.5194/gmd-10-1903-2017, 2017a.

Martens, B., Miralles, D. G., Lievens, H., van der Schalie, R., de Jeu, R. A. M., Fernández-Prieto, D., Beck, H. E., Dorigo, W. A., and Verhoest, N. E. C.: GLEAM v3: satellite-based land evaporation and root-zone soil moisture, Geosci. Model Dev., 10, 1903-1925, 10.5194/gmd-10-1903-2017, 2017b.

Meng, S. S., Xie, X. H., Zhu, B. W., and Wang, Y. B.: The relative contribution of vegetation greening to the hydrological cycle in the Three-North region of China: A modelling analysis, Journal of Hydrology, 591, 10.1016/j.jhydrol.2020.125689, 2020.

Miralles, D. G., Holmes, T. R. H., De Jeu, R. A. M., Gash, J. H., Meesters, A., and Dolman, A. J.: Global land-surface evaporation estimated from satellite-based observations, Hydrology and Earth System Sciences, 15, 453-469, 10.5194/hess-15-453-2011, 2011.

Mladenova, I. E., Bolten, J. D., Crow, W. T., Sazib, N., Cosh, M. H., Tucker, C. J., and Reynolds, C.: Evaluating the Operational Application of SMAP for Global Agricultural Drought Monitoring, IEEE Journal of Selected Topics in Applied Earth Observations and Remote Sensing, 12, 3387-3397, 10.1109/JSTARS.2019.2923555, 2019.

Novick, K. A., Ficklin, D. L., Stoy, P. C., Williams, C. A., Bohrer, G., Oishi, A. C., Papuga, S. A., Blanken, P. D., Noormets, A., Sulman, B. N., Scott, R. L., Wang, L., and Phillips, R. P.: The increasing importance of atmospheric demand for ecosystem water and carbon fluxes, Nature Climate Change, 6, 1023-1027, 10.1038/nclimate3114, 2016.

Oren, R., Sperry, J. S., Katul, G. G., Pataki, D. E., Ewers, B. E., Phillips, N., and Schäfer, K. V. R.: Survey and synthesis of intra- and interspecific variation in stomatal sensitivity to vapour pressure deficit, Plant Cell and Environment, 22, 1515-1526, 1999.

Pascolini-Campbell, M., Reager, J. T., Chandanpurkar, H. A., and Rodell, M.: RETRACTED ARTICLE: A 10 per cent increase in global land evapotranspiration from 2003 to 2019, Nature, 593, 543-547, 10.1038/s41586-021-03503-5, 2021.

Qing, Y. M., Wang, S., Yang, Z. L., Gentine, P., Zhang, B., and Alexander, J.: Accelerated soil drying linked to increasing evaporative demand in wet regions, Npj Climate and Atmospheric Science, 6, 10.1038/s41612-023-00531-y, 2023.

Qiu, B., Chen, G., Tang, Z., Lu, D., Wang, Z., and Chen, C.: Assessing the Three-North Shelter Forest Program in China by a novel framework for characterizing vegetation changes, ISPRS Journal of Photogrammetry and Remote Sensing, 133, 75-88, https://doi.org/10.1016/j.isprsjprs.2017.10.003, 2017.

Qiu, L., Wu, Y., Shi, Z., Yu, M., Zhao, F., and Guan, Y.: Quantifying spatiotemporal variations in soil moisture driven by vegetation restoration on the Loess Plateau of China, Journal of Hydrology, 600, 126580, https://doi.org/10.1016/j.jhydrol.2021.126580, 2021.

Roderick, M. L., Rotstayn, L. D., Farquhar, G. D., and Hobbins, M. T.: On the attribution of changing pan evaporation, Geophysical Research Letters, 34, 10.1029/2007gl031166, 2007.

Ruichen, M., Jinxi, S., Bin, T., Wenjin, X., Feihe, K., Haotian, S., and Yuxin, L.: Vegetation variation regulates soil moisture sensitivity to climate change on the Loess Plateau, Journal of Hydrology, 617, 128763, https://doi.org/10.1016/j.jhydrol.2022.128763, 2023a.

Ruichen, M., Jinxi, S., Bin, T., Wenjin, X., Feihe, K., Haotian, S., and Yuxin, L.: Vegetation variation regulates soil moisture sensitivity to climate change on the Loess Plateau, Journal of Hydrology, 617, 10.1016/j.jhydrol.2022.128763, 2023b.

https://doi.org/10.5194/egusphere-2025-2828
Preprint. Discussion started: 8 July 2025
© Author(s) 2025. CC BY 4.0 License.

Seneviratne, S. I., Corti, T., Davin, E. L., Hirschi, M., Jaeger, E. B., Lehner, I., Orlowsky, B., and Teuling, A. J.: Investigating soil moisture–climate interactions in a changing climate: A review, Earth-Science Reviews, 99, 125-161, https://doi.org/10.1016/j.earscirev.2010.02.004, 2010a.

Seneviratne, S. I., Corti, T., Davin, E. L., Hirschi, M., Jaeger, E. B., Lehner, I., Orlowsky, B., and Teuling, A. J.: Investigating soil moisture-climate interactions in a changing climate: A review, Earth-Science Reviews, 99, 125-161, 10.1016/j.earscirev.2010.02.004, 2010b.

Shi, S. Y., Wang, P., and Yu, J. J.: Vegetation greening and climate change promote an increase in evapotranspiration across Siberia, Journal of Hydrology, 610, 10.1016/j.jhydrol.2022.127965, 2022.

Sinclair, T. R., Devi, J., Shekoofa, A., Choudhary, S., Sadok, W., Vadez, V., Riar, M., and Rufty, T.: Limited-transpiration response to high vapor pressure deficit in crop species, Plant Science, 260, 109-118, https://doi.org/10.1016/j.plantsci.2017.04.007, 2017.

Sklar, M. J.: Fonctions de repartition a n dimensions et leurs marges,

Smith, T. and Boers, N.: Global vegetation resilience linked to water availability and variability, Nature Communications, 14, 498, 10.1038/s41467-023-36207-7, 2023.

Strassburg, B. B. N., Iribarrem, A., Beyer, H. L., Cordeiro, C. L., Crouzeilles, R., Jakovac, C. C., Braga Junqueira, A., Lacerda, E., Latawiec, A. E., Balmford, A., Brooks, T. M., Butchart, S. H. M., Chazdon, R. L., Erb, K.-H., Brancalion, P., Buchanan, G., Cooper, D., Díaz, S., Donald, P. F., Kapos, V., Leclère, D., Miles, L., Obersteiner, M., Plutzar, C., de M. Scaramuzza, C. A., Scarano, F. R., and Visconti, P.: Global priority areas for ecosystem restoration, Nature, 586, 724-729, 10.1038/s41586-020-2784-9, 2020.

Su, L., Miao, C. Y., Duan, Q. Y., Lei, X. H., and Li, H.: Multiple-Wavelet Coherence of World's Large Rivers With Meteorological Factors and Ocean Signals, Journal of Geophysical Research-Atmospheres, 124, 4932-4954, 10.1029/2018jd029842, 2019.

Sun, S. L., Liu, Y. B., Chen, H. S., Ju, W. M., Xu, C. Y., Liu, Y., Zhou, B. T., Zhou, Y., Zhou, Y. L., and Yu, M.: Causes for the increases in both evapotranspiration and water yield over vegetated mainland China during the last two decades, Agricultural and Forest Meteorology, 324, 10.1016/j.agrformet.2022.109118, 2022.

Tang, Y. and Tang, Q. H.: Variations and influencing factors of potential evapotranspiration in large Siberian river basins during 1975-2014, Journal of Hydrology, 598, 10.1016/j.jhydrol.2021.126443, 2021.

Thomson, R., Barclay, D., and Higgins, C.: The partial least squares approach to causal modeling: Personal computer adoption and use as an illustration, Technology Studies: Special Issue on Research Methodology, 2, 284-324, 1995.

Tietjen, B., Schlaepfer, D. R., Bradford, J. B., Lauenroth, W. K., Hall, S. A., Duniway, M. C., Hochstrasser, T., Jia, G., Munson, S. M., Pyke, D. A., and Wilson, S. D.: Climate change-induced vegetation shifts lead to more ecological droughts despite projected rainfall increases in many global temperate drylands, Global Change Biology, 23, 2743-2754, 10.1111/gcb.13598, 2017.

Torrence, C. and Compo, G. P.: A Practical Guide to Wavelet Analysis, Bulletin of the American Meteorological Society, 79, 61-78, 1998.

Vereecken, H., Huisman, J. A., Pachepsky, Y., Montzka, C., van der Kruk, J., Bogena, H., Weihermüller, L., Herbst, M., Martinez, G., and Vanderborght, J.: On the spatio-temporal dynamics of soil moisture at the field scale, Journal of Hydrology, 516, 76-96, 10.1016/j.jhydrol.2013.11.061, 2014.

Vereecken, H., Amelung, W., Bauke, S. L., Bogena, H., Brüggemann, N., Montzka, C., Vanderborght, J., Bechtold, M., Blöschl, G., Carminati, A., Javaux, M., Konings, A. G., Kusche, J., Neuweiler, I., Or, D., Steele-Dunne, S., Verhoef, A., Young, M., and Zhang, Y.: Soil hydrology in the Earth system, Nature Reviews Earth & Environment, 3, 573-587, 10.1038/s43017-022-00324-6, 2022.

Wang, L. X., Good, S. P., and Caylor, K. K.: Global synthesis of vegetation control on evapotranspiration partitioning, Geophysical Research Letters, 41, 6753-6757, 10.1002/2014gl061439, 2014.

https://doi.org/10.5194/egusphere-2025-2828
Preprint. Discussion started: 8 July 2025
© Author(s) 2025. CC BY 4.0 License.

Wang, X. Y., Wang, T., Liu, D., Guo, H., Huang, H. B., and Zhao, Y. T.: Moisture-induced greening of the South Asia over the past three decades, Global Change Biology, 23, 4995-5005, 10.1111/gcb.13762, 2017.

Wang, Y., Zhang, Y., Yu, X., Jia, G., Liu, Z., Sun, L., Zheng, P., and Zhu, X.: Grassland soil moisture fluctuation and its relationship with evapotranspiration, Ecological Indicators, 131, 108196, https://doi.org/10.1016/j.ecolind.2021.108196, 2021.

Wang, Z., Fu, B., Wu, X., Li, Y., Feng, Y., Wang, S., Wei, F., and Zhang, L.: Vegetation resilience does not increase consistently with greening in China's Loess Plateau, Communications Earth & Environment, 4, 336, 10.1038/s43247-023-01000-3, 2023.

Wei, Z. W., Yoshimura, K., Wang, L. X., Miralles, D. G., Jasechko, S., and Lee, X. H.: Revisiting the contribution of transpiration to global terrestrial evapotranspiration, Geophysical Research Letters, 44, 2792-2801, 10.1002/2016gl072235, 2017.

Westland, J. C.: Partial Least Squares Path Analysis, in: Structural Equation Models: From Paths to Networks, edited by: Westland, J. C., Springer International Publishing, Cham, 23-46, 10.1007/978-3-319-16507-3_3, 2015.

Wu, H., Su, X., Huang, S., Singh, V. P., Zhou, S., Tan, X., and Hu, X.: Decreasing dynamic predictability of global agricultural drought with warming climate, Nature Climate Change, 10.1038/s41558-025-02289-y, 2025.

Xiao, Z. Q., Liang, S. L., and Jiang, B.: Evaluation of four long time-series global leaf area index products, Agricultural and Forest Meteorology, 246, 218-230, 10.1016/j.agrformet.2017.06.016, 2017.

Xiao, Z. Q., Liang, S. L., Wang, J. D., Xiang, Y., Zhao, X., and Song, J. L.: Long-Time-Series Global Land Surface Satellite Leaf Area Index Product Derived From MODIS and AVHRR Surface Reflectance, Ieee Transactions on Geoscience and Remote Sensing, 54, 5301-5318, 10.1109/tgrs.2016.2560522, 2016.

Xie, X. H., Liang, S. L., Yao, Y. J., Jia, K., Meng, S. S., and Li, J.: Detection and attribution of changes in hydrological cycle over the Three-North region of China: Climate change versus afforestation effect, Agricultural and Forest Meteorology, 203, 74-87, 10.1016/j.agrformet.2015.01.003, 2015.

Xu, L., Gao, G. Y., Wang, X. F., and Fu, B. J.: Distinguishing the effects of climate change and vegetation greening on soil moisture variability along aridity gradient in the drylands of northern China, Agricultural and Forest Meteorology, 343, 10.1016/j.agrformet.2023.109786, 2023.

Yang, F., Huang, M. B., Li, C. H., Wu, X. F., Guo, T. Q., and Zhu, M. Y.: Changes in soil moisture and organic carbon under deep-rooted trees of different stand ages on the Chinese Loess Plateau, Agriculture Ecosystems & Environment, 328, 10.1016/j.agee.2022.107855, 2022.

Yang, J., Xu, X. L., Liu, M. X., Xu, C. H., Luo, W., Song, T. Q., Du, H., and Kiely, G.: Effects of Napier grass management on soil hydrologic functions in a karst landscape, southwestern China, Soil & Tillage Research, 157, 83-92, 10.1016/j.still.2015.11.012, 2016.

Yang, J., Xu, X., Liu, M., Xu, C., Zhang, Y., Luo, W., Zhang, R., Li, X., Kiely, G., and Wang, K.: Effects of "Grain for Green" program on soil hydrologic functions in karst landscapes, southwestern China, Agriculture, Ecosystems & Environment, 247, 120-129, https://doi.org/10.1016/j.agee.2017.06.025, 2017.

Yang, L., Wei, W., Chen, L. D., Chen, W. L., and Wang, J. L.: Response of temporal variation of soil moisture to vegetation restoration in semi-arid Loess Plateau, China, Catena, 115, 123-133, 10.1016/j.catena.2013.12.005, 2014.

Yang, W., Jin, F., Si, Y., and Li, Z.: Runoff change controlled by combined effects of multiple environmental factors in a headwater catchment with cold and arid climate in northwest China, Science of The Total Environment, 756, 143995, https://doi.org/10.1016/j.scitotenv.2020.143995, 2021.

Yang, Z., Gong, J., Wang, S., Jin, T., and Wang, Y.: Shifts bidirectional dependency between vegetation greening and soil moisture over the past four decades in China, Science of The Total Environment, 897, 166388, https://doi.org/10.1016/j.scitotenv.2023.166388, 2023.

https://doi.org/10.5194/egusphere-2025-2828
Preprint. Discussion started: 8 July 2025
© Author(s) 2025. CC BY 4.0 License.

Ye, L. P., Fang, L. C., Shi, Z. H., Deng, L., and Tan, W. F.: Spatio-temporal dynamics of soil moisture driven by 'Grain for Green' program on the Loess Plateau, China, Agriculture Ecosystems & Environment, 269, 204-214, 10.1016/j.agee.2018.10.006, 2019.

Yuan, X., Wang, Y., Ji, P., Wu, P., Sheffield, J., and Otkin, J. A.: A global transition to flash droughts under climate change, Science, 380, 187-191, doi:10.1126/science.abn6301, 2023.

Zani, D., Crowther, T. W., Mo, L., Renner, S. S., and Zohner, C. M.: Increased growing-season productivity drives earlier autumn leaf senescence in temperate trees, Science, 370, 1066-1071, 10.1126/science.abd8911, 2020.

Zeng, Z., Peng, L., and Piao, S.: Response of terrestrial evapotranspiration to Earth's greening, Current Opinion in Environmental Sustainability, 33, 9-25, https://doi.org/10.1016/j.cosust.2018.03.001, 2018.

Zeng, Z. Z., Piao, S. L., Li, L. Z. X., Zhou, L. M., Ciais, P., Wang, T., Li, Y., Lian, X., Wood, E. F., Friedlingstein, P., Mao, J. F., Estes, L. D., Myneni, R. B., Peng, S. S., Shi, X. Y., Seneviratne, S. I., and Wang, Y. P.: Climate mitigation from vegetation biophysical feedbacks during the past three decades, Nature Climate Change, 7, 432-+, 10.1038/nclimate3299, 2017.

Zhang, K., Xie, X., Zhu, B., Meng, S., and Yao, Y.: Unexpected groundwater recovery with decreasing agricultural irrigation in the Yellow River Basin, Agricultural Water Management, 213, 858-867, https://doi.org/10.1016/j.agwat.2018.12.009, 2019a.

Zhang, M., Yuan, X., Zeng, Z., Pan, M., Wu, P., Xiao, J., and Keenan, T. F.: A pronounced decline in northern vegetation resistance to flash droughts from 2001 to 2022, Nature Communications, 16, 2984, 10.1038/s41467-025-58253-z, 2025.

Zhang, W., Wei, F., Horion, S., Fensholt, R., Forkel, M., and Brandt, M.: Global quantification of the bidirectional dependency between soil moisture and vegetation productivity, Agricultural and Forest Meteorology, 313, 108735, https://doi.org/10.1016/j.agrformet.2021.108735, 2022a.

Zhang, W. M., Wei, F. L., Horion, S., Fensholt, R., Forkel, M., and Brandt, M.: Global quantification of the bidirectional dependency between soil moisture and vegetation productivity, Agricultural and Forest Meteorology, 313, 10.1016/j.agrformet.2021.108735, 2022b.

Zhang, Y., Keenan, T. F., and Zhou, S.: Exacerbated drought impacts on global ecosystems due to structural overshoot, Nature Ecology & Evolution, 5, 1490-1498, 10.1038/s41559-021-01551-8, 2021.

Zhang, Y., Xu, X., Li, Z., Liu, M., Xu, C., Zhang, R., and Luo, W.: Effects of vegetation restoration on soil quality in degraded karst landscapes of southwest China, Science of The Total Environment, 650, 2657-2665, https://doi.org/10.1016/j.scitotenv.2018.09.372, 2019b.

Zhang, Y. Q., Liu, C. M., Tang, Y. H., and Yang, Y. H.: Trends in pan evaporation and reference and actual evapotranspiration across the Tibetan Plateau, Journal of Geophysical Research-Atmospheres, 112, 10.1029/2006jd008161, 2007.

Zhao, F. B., Ma, S., Wu, Y. P., Qiu, L. J., Wang, W. K., Lian, Y. Q., Chen, J., and Sivakumar, B.: The role of climate change and vegetation greening on evapotranspiration variation in the Yellow River Basin, China, Agricultural and Forest Meteorology, 316, 10.1016/j.agrformet.2022.108842, 2022.

Zhao, J., Huang, S., Huang, Q., Leng, G., Wang, H., and Li, P.: Watershed water-energy balance dynamics and their association with diverse influencing factors at multiple time scales, Science of The Total Environment, 711, 135189, https://doi.org/10.1016/j.scitotenv.2019.135189, 2020.

Zhao, W., Sánchez, N., Lu, H., and Li, A.: A spatial downscaling approach for the SMAP passive surface soil moisture product using random forest regression, Journal of Hydrology, 563, 1009-1024, https://doi.org/10.1016/j.jhydrol.2018.06.081, 2018.

Zhou, S., Williams, A. P., Lintner, B. R., Berg, A. M., Zhang, Y., Keenan, T. F., Cook, B. I., Hagemann, S., Seneviratne, S. I., and Gentine, P.: Soil moisture-atmosphere feedbacks mitigate declining water availability in drylands, Nature Climate Change, 11, 38-+, 10.1038/s41558-020-00945-z, 2021a.

https://doi.org/10.5194/egusphere-2025-2828
Preprint. Discussion started: 8 July 2025
© Author(s) 2025. CC BY 4.0 License.

943 Zhou, S., Williams, A. P., Lintner, B. R., Berg, A. M., Zhang, Y., Keenan, T. F., Cook, B. I., Hagemann, S.,
944 Seneviratne, S. I., and Gentine, P.: Soil moisture–atmosphere feedbacks mitigate declining water availability in
945 drylands, Nature Climate Change, 11, 38-44, 10.1038/s41558-020-00945-z, 2021b.
946 Zhu, Z. C., Piao, S. L., Myneni, R. B., Huang, M. T., Zeng, Z. Z., Canadell, J. G., Ciais, P., Sitch, S., Friedlingstein,
947 P., Arneth, A., Cao, C. X., Cheng, L., Kato, E., Koven, C., Li, Y., Lian, X., Liu, Y. W., Liu, R. G., Mao, J. F., Pan,
948 Y. Z., Peng, S. S., Penuelas, J., Poulter, B., Pugh, T. A. M., Stocker, B. D., Viovy, N., Wang, X. H., Wang, Y. P.,
949 Xiao, Z. Q., Yang, H., Zaehle, S., and Zeng, N.: Greening of the Earth and its drivers, Nature Climate Change, 6,
950 791-+, 10.1038/nclimate3004, 2016.
951 Zohaib, M., Kim, H., and Choi, M.: Evaluating the patterns of spatiotemporal trends of root zone soil moisture in
952 major climate regions in East Asia, Journal of Geophysical Research: Atmospheres, 122, 7705-7722,
953 https://doi.org/10.1002/2016JD026379, 2017.
954 Zscheischler, J. and Seneviratne, S. I.: Dependence of drivers affects risks associated with compound events,
955 Science Advances, 3, 10.1126/sciadv.1700263, 2017.
956